γδ T cells mediate a requisite portion of a wound healing response triggered by cutaneous poxvirus infection

Short Title: γδ T cells mediate wound healing after viral skin infection

Irene E. Reider[1], Eugene Lin[1], Tracy E. Krouse[1], Nikhil J. Parekh[1], Amanda M. Nelson[2] and Christopher C. Norbury[1*],

[1]Department of Microbiology and Immunology

[2]Department of Dermatology,

Pennsylvania State University College of Medicine, Hershey, Pennsylvania, United States of America

*Corresponding author

ccn1@psu.edu (CCN)

Abstract

Infection at peripheral sites, such as the skin, activates local innate immune defenses tasked with limiting spread of the pathogen while preserving tissue integrity. T cells bearing γδ T Cell Receptors (TCR), which comprise multiple phenotypically distinct subtypes of cells, reside in normal skin, where they shape immunity to cutaneous infection, prior to onset of an adaptive immune response by conventional αβ $CD4^+$ (T_{CD4+}) and $CD8^+$ (T_{CD8+}) T cells. The mechanisms used by γδ T cells to control virus replication and tissue pathology following cutaneous infection are unknown, so we examined the role of γδ T cells in the response to cutaneous infection with vaccinia virus (VACV). Resident γδ T cells in the skin expanded and combined with recruited γδ T cells to control the pathology observed after cutaneous VACV infection. However, we observed no defect in control of local virus replication or increased systemic spread in mice lacking γδ T cells, despite induction of a cytolytic response in a specialized subset of resident γδ T cells. While examining γδ T cell-mediated control of tissue pathology following cutaneous VACV infection, we identified a unique wound healing signature associated with cutaneous virus infection that has features that are common to, but also features that antagonize, the sterile cutaneous wound healing response. Typically, tissue repair is thought to occur only after clearance of a pathogen, but the viral wound healing signature was evident prior to the peak of virus replication in the skin. Resident and recruited γδ T cells contributed to this wound healing signature through induction of multiple cytokines and growth factors required for efficient wound closure. Therefore, γδ T cells are early mediators of the wound healing response following cutaneous virus infection and are likely important in maintenance of skin barrier function and prevention of secondary bacterial infection.

Author Summary

γδ T cells resident in the skin are among the first immune cell types positioned to be able to respond to a virus infection of the skin. Therefore, it was assumed that these cells in the skin play a role similar to their role after widespread infection throughout the body, namely to kill virus infected cells and slow virus replication and spread. However, we found no role for γδ T cells in control of virus replication after infection of the skin. Rather, the γδ T cells functioned as a critical component of a previously unrecognized wound healing response that is started early after virus infection of the skin, and occurs at the same time as the immune response that aims to clear the virus. This study is the first to describe both the early wound healing response after virus infection, and the role of γδ T cells in that response, and this information could allow manipulation of this response to decrease secondary bacterial infection and change scarring after virus skin infections.

Introduction

Skin resident γδ T cells are among the first dedicated effector immune cells to encounter a cutaneous virus infection, and have the potential to alter the course of the infection prior to the expansion and infiltration of conventional αβ T cells (both T_{CD4+} and T_{CD8+}). Therefore, we sought to establish the role of skin resident and skin recruited γδ T cells upon control of a local cutaneous virus infection, along with their impact on systemic spread of the virus and the local pathology caused by the infection. Vaccinia virus (VACV) is an orthopoxvirus that was the most successful vaccine ever used (protecting against smallpox caused by variola virus) and now forms the basis for numerous clinical vaccine vectors. The efficacy of vaccination with VACV depends on cutaneous infection and damage [1]. There are numerous experimental and clinical indications that a cutaneous infection is the natural route of infection with VACV [2-4]. VACV is also related to both the skin-tropic orf virus, a prominent poxviral veterinary pathogen, and molluscum contagiosum, a poxvirus which infects tens of millions around the world and which can cause severe infections in immunocompromised patients [5, 6]. Thus, understanding the mechanisms and interactions between VACV and the host will provide insights about similar interactions between human and veterinary pathogens, and may identify therapeutic targets that allow manipulation of the host response, or which ameliorate pathology following infection. After systemic infection, γδ T cells exhibit cytolytic control over the replication and spread of VACV infection [7-10], but our previous work has identified key differences in how the immune system responds to control viruses after systemic infection versus the more relevant peripheral cutaneous infection. In particular, we have identified both cellular and molecular mechanisms that are induced following cutaneous VACV infection which act to control the extent of local pathology measured by lesion size and tissue loss, but which do not have large effects upon local VACV replication [11-13]. Therefore, we sought to examine the role of skin resident and skin recruited γδ T cells after cutaneous VACV infection.

Adult murine skin contains γδ T cell subsets that reside in both the epidermis and dermis and are distinguished by the Vγ TCR chain expression. Dendritic epidermal T cells (DETC) express the Vγ3 TCR chain (Garman and Raulet nomenclature [14]), whereas dermal γδ T cells express either Vγ2 or Vγ4 [15, 16]. Tissue resident cells in the skin reside among epithelial cells and are distinguished by expression of the epithelial cell adhesion molecule (Ep-CAM, CD326). In various skin pathologies γδ T cell subsets each have distinct functions, including production of IFN-γ [17-21] or IL-17A [22-25], recruitment of myeloid cells [26, 27], lysis of virus infected cells [18, 28, 29] and pro-wound healing functions [26, 30-44]. Therefore, it is likely that each resident γδ T cell type, along with recruited γδ T cells, has a differential ability to be activated, and correspondingly, a different function, following cutaneous VACV infection. In addition, γδ T cell phenotype and function are also influenced by the local microbiome [45], adding an additional wrinkle to any phenotype or function observed in uninfected or virus-infected skin.

In this study, we found that neither resident nor recruited γδ T cells are involved in the local control of VACV replication, or in the control of spread of VACV systemically, despite Vγ3 DETC displaying a cytolytic phenotype in response to cutaneous VACV infection. However, in the absence of γδ T cells, VACV infection induced a marked increase in tissue pathology over that observed in a WT situation. Neither tissue resident nor recruited γδ T cells appear to modulate any of the tissue protective functions (e.g., recruitment of myeloid cell populations, production of reactive oxygen species or Type I interferon) we have previously described as important during cutaneous VACV infection [11-13]. However, while investigating the mechanisms by which γδ T cells impact local tissue pathology we discovered induction of a unique wound healing signature induced early after VACV infection. This signature bears hallmarks of the classical wound healing response described after sterile wounding, but the viral wound healing response also displays some marked differences from the sterile response. Notably, this wound healing signature is induced early after virus infection, prior to the peak of virus replication in the skin, in contrast to

the accepted paradigm, in which wound healing begins only after virus clearance [46, 47]. Our data indicate that γδ T cells mediate a requisite component of this local viral wound healing response by producing, or inducing the production of, IL-17A, IL-22, IL-10, keratinocyte growth factor (KGF) and fibroblast growth factor 9 (FGF9). Therefore, the actions of γδ T cells are likely crucial in the closure of wounded skin following cutaneous virus infection, the prevention of secondary bacterial infections within the virus induced lesions, and the maintenance of the crucial barrier function of the skin.

Results

Infected and uninfected γδ T cells in the skin are present in the foci of VACV infection and expand early after infection.

VACV is a widely-used vaccine vector, and dermal administration of the vaccine most effectively induces a protective adaptive immune response [1]. However, the major complications of immunization with VACV arise either from uncontrolled virus replication, or from uncontrolled inflammation at the site of infection. The immune cells that are present in the skin at the site of infection likely play a vital role in local control of virus replication or inflammation, or both, prior to the recruitment of innate and adaptive effector cells. γδ T cells reside in the dermis and epidermis of the skin [48], and mice lacking γδ T cells are deficient in control of systemic VACV infection [7-10] and other poxviruses [49-53]. To visualize the interaction of γδ T cells and VACV within the skin, we inoculated WT mice with VACV-GFP using a bifurcated needle, a method that both generates easily identifiable foci of infection, and mimics the route of human immunization with VACV. We harvested ear tissue 4d after infection and stained tissue sections for the presence of TCRδ using antibodies. By immunofluorescence microscopy, we observed significant numbers of TCRδ$^+$ γδ T cells that display typical dendritic morphology within the GFP$^+$ VACV lesion, as well as some cells localized along the boundaries of the lesions (**Fig. 1A**). No staining for TCRδ was seen in control TCRδ$^{-/-}$ mice (**Fig. 1B**). Thus, γδ T cells are in a position to sense VACV infection, potentially lyse VACV-infected cells, and orchestrate the subsequent innate and adaptive immune response. VACV appeared to infect some γδ T cells within the infected foci. To confirm that VACV did infect γδ T cells in the skin, we infected mice intradermally with VACV, harvested ears on d4 post-infection and analyzed γδ T cells by flow cytometry. This route of infection results in a localized infection in immunocompetent mice [3, 4]. We observed that a proportion (~11-15%) of

γδ T cells in the ear expressed GFP after infection with VACV-GFP, indicating that these cells become infected with VACV (**Fig. 1C**).

To dissect γδ T cell responses in the skin following VACV infection, we stained single cell suspensions harvested from infected ears with antibodies to TCRδ, as well as with antibodies to conventional αβ T cells, and performed flow cytometry analysis using the gating strategy outlined in **Figure 1D**. As observed in a previous study [54], the numbers of γδ T cells increased early following infection (> 2-fold) and peaked at d2 post-infection (p.i.) (**Fig. 1E**). The expansion in number of γδ T cells appeared to represent an expansion or recruitment of all of the subsets of these cells. Notably, γδ T cells were the major lymphoid population in the VACV-infected ear until d4-5 p.i. (**Fig. 1E**), as NK cells are not recruited to the site of infection [11]. In addition, conventional T_{CD4+} and T_{CD8+} were recruited to the ear from the naïve precursor pool but did not surpass numbers of γδ T cells until at least d5 post-infection (**Fig. 1E**). Indeed, although numerous studies have examined the T_{CD8+} response to VACV following infection of the skin [55, 56], these cells were in the minority compared to T_{CD4+} cells, which accumulate with similar kinetics and persist for much longer following infection (**Fig. 1E**).

To further define the γδ T cell populations in infected and uninfected skin, we quantified the numbers of $V\gamma3^+$ DETCs [14] and $V\gamma2^+$ dermal γδ T cells [15, 16] or $V\gamma3^-V\gamma2^-$ γδ T cells. After VACV infection, staining with antibodies to Vγ3 and Vγ2 TCR chains revealed that DETC, which were consistently more abundant than other γδ T cell subsets, nearly doubled in number by d2 p.i., and then underwent a drastic contraction before recovering following resolution of infection (**Fig. 1F**). In contrast, $V\gamma2^+$ dermal γδ T cell numbers peaked somewhat later around d4 p.i., but underwent a slow, gradual contraction (**Fig. 1F**). On the other hand, the more abundant $V\gamma2^-V\gamma3^-$ dermal γδ T cell population, which likely expresses the Vγ4 chain [16], displayed similar patterns of expansion, contraction, and recovery as DETCs (**Fig. 1F**). The distinct expansion and

158 recruitment kinetics of γδ T cell populations suggests that each population may have a distinct
159 function and role that contributes to the overall successful host response to viral infection.
160
161 ***A distinct γδ T cell subset displays cytolytic function after VACV infection, but does not***
162 ***control local virus replication or systemic spread.***
163 γδ T cells exhibit a variety of functions depending on the subtype, the stage of life at which
164 they develop, and sub-anatomical location [57]. As γδ T cells have previously been proposed to
165 mediate antiviral immunity via cytolytic activity [18, 28, 29], we initially examined the ability of γδ
166 T cell subsets (Vγ3$^+$ DETC, Vγ2$^+$ dermal γδ T cells or Vγ3$^-$Vγ2$^-$ γδ T cells), conventional T_{CD8+} or
167 T_{CD4+} to degranulate in response to a broad activation signal, PMA/ionomycin treatment (**Fig. 2A**).
168 Degranulation, measured via cell-surface expression of the endosomal marker CD107a in
169 response to PMA/ionomycin, was measured on d4 and d8 post-infection, except in T_{CD8+}, which
170 were only present in the VACV-infected ear at d8 post-infection. We found minor cell surface
171 staining with an anti-CD107a antibody after PMA/ionomycin treatment in T_{CD4+} and Vγ3$^+$ DETC
172 on d8 post-infection, but a marked activation-induced degranulation by the majority of Vγ3$^+$ DETC
173 4 days after VACV infection (**Fig. 2A**). We saw only background levels of CD107a staining in the
174 other cell types examined, either with or without of PMA/ionomycin activation. Effective cytolysis
175 of virus-infected cells often requires the secretion of serine proteases, such as granzyme B (GzB),
176 during degranulation [58]. Therefore, we also examined intracellular expression of GzB by Vγ3$^+$
177 DETC, Vγ2$^+$ dermal γδ T cells or Vγ3$^-$Vγ2$^-$ γδ T cells, as well as by conventional T_{CD8+} or T_{CD4+}, as
178 above (**Fig. 2B**). On d8 post-infection, approximately one-third of Vγ3$^+$ DETC, about one-half of
179 T_{CD4+} and almost all of the T_{CD8+} expressed GzB, indicating they likely display cytolytic activity
180 against VACV-infected cells (**Fig. 2B**). Earlier after infection, at d4, a similar proportion of about
181 one-third of Vγ3$^+$ DETC expressed GzB, and a small number of T_{CD4+} also had cytolytic capability
182 (**Fig. 2B**). However, the majority of γδ T cells did not express GzB (**Fig. 2B**). Taken together,

these data indicate that, of the γδ T cells present, only Vγ3^{+} DETC likely have the capability to directly kill VACV-infected cells in the ear.

The observation that DETC possess cytolytic activity after VACV infection drove us to examine whether γδ T cells play a direct antiviral role following cutaneous infection, as proposed previously following systemic infection [7-10]. We examined VACV titers in the ear of WT and TCRδ$^{-/-}$ mice, which lack γδ T cells, at d5 post-infection (**Fig. 2C**), a time point corresponding to the peak of virus replication [11] and at d8 post-infection (**Fig. 2D**), a time point before tissue loss occurs. VACV titers in the ear in TCRδ$^{-/-}$ versus WT mice displayed only small (~1.5 fold) differences (**Fig. 2C, D**), indicating that γδ T cells do not directly or indirectly contribute significantly to the control of local cutaneous VACV replication.

A major function of the initial immune response to a peripheral virus infection is to contain the infection at the initial site, prior to recruitment of innate and adaptive effector cells which then mediate clearance of the infection. Dermal VACV infection remains primarily localized to the ear following infection [3], but removal of various immune components can allow systemic spread to the primary site of VACV replication, the ovaries [12]. However, we found no significant spread of VACV to the ovaries of TCRδ$^{-/-}$ mice, indicating that γδ T cells are not likely to play a critical role in restricting systemic spread of VACV (**Fig. 2C, D**). Therefore, γδ T cells are not required to control local VACV replication, or systemic spread of VACV.

Mice infected in the ears with VACV develop visible lesions that undergo necrosis and the necrotic tissue is then lost [3, 4]. We have previously described a role for two recruited populations of monocytes, production of reactive oxygen species and local Type I IFN production in control of the severity of pathology observed following dermal VACV infection [11-13]. However, none of the factors mentioned above are involved in control of local VACV replication or spread from the original site of infection. Therefore, we sought to examine whether γδ T cells in the skin may play a similar role in controlling the severity of pathology following VACV infection, without displaying

208 a role in control over local VACV replication. By measuring tissue swelling, the dimensions of the
209 lesions and ensuing tissue loss in WT and TCR$\delta^{-/-}$ mice, we assessed the extent of tissue damage
210 following VACV infection. TCR$\delta^{-/-}$ mice exhibited no change in swelling of VACV-infected ear
211 tissue in the 6 days following the initial infection when compared to that observed in WT mice
212 (**Fig. 2E**). However, TCR$\delta^{-/-}$ mice subsequently displayed visibly larger skin lesions than their
213 VACV-infected WT counterparts on d8 post-infection (**Fig. 2 F, G**) and this was quantified to
214 indicate a statistically significant change in lesion size from d6-14 post-infection (**Fig. 2H**).
215 Correspondingly, there was also a visible and quantifiable acceleration and increase in severity
216 of tissue loss in TCR$\delta^{-/-}$ mice compared to their WT counterparts (**Fig. 2 I-K**). Taken together,
217 these data indicate that $\gamma\delta$ T cells control the severity and progression of tissue pathology at the
218 cutaneous site of VACV infection without playing a role in the control of local VACV replication.
219
220 ***$\gamma\delta$ T cell responses to VACV do not influence the local or systemic T_{CD8+} response to VACV.***
221 The observation that $\gamma\delta$ T cells do not control VACV replication or spread, but do
222 ameliorate exacerbated tissue loss following VACV infection, suggested that an overly zealous
223 local immune host response in the absence of $\gamma\delta$ T cells could cause an increase in local necrosis
224 in the absence of an increase in VACV replication. Such an observation would indicate an
225 immunoregulatory or immunosupressive role for $\gamma\delta$ T cells. To test this we examined the effect of
226 $\gamma\delta$ T cells upon multiple components of the cutaneous immune response following VACV infection.
227 T_{CD8+} are a vital component of antiviral immunity that are recruited to the VACV-infected ear (**Fig.**
228 **1E**) and localize around the periphery of the VACV lesion, thus preventing spread of the virus 4d
229 after infection [12, 55, 59]. Therefore, we sought to examine a potential role for $\gamma\delta$ T cells in the
230 priming, recruitment, localization or subsequent function of T_{CD8+} in the anti-VACV response. We
231 found no differences in the numbers of T_{CD8+} recruited to the ear either 5d (**Fig. 3A**) or 8d (**Fig.**
232 **3B**) after cutaneous VACV infection of WT or TCR$\delta^{-/-}$ mice. We then examined the localization of

233 T_{CD8+} relative to VACV-infected cells after VACV-GFP infection of WT or TCR$\delta^{-/-}$ mice (**Fig. 3C,**
234 **D**). In both sets of mice we observed T_{CD8+} around the periphery of the VACV lesion (**Fig. 3C, D**),
235 indicating that there was no defect in T_{CD8+} localization in the absence of $\gamma\delta$ T cells. Next, we
236 examined the production of IFN-γ and TNFα by T_{CD8+} in the VACV-infected ears of both mouse
237 strains on d5 (**Fig. 3E**) or d8 (**Fig. 3F**) post-infection. We found, on both d5 and d8 post-infection,
238 that cytokine production by T_{CD8+} directly *ex vivo* was indistinguishable in WT vs. TCR$\delta^{-/-}$ mice
239 (**Fig. 3E, F**). These data suggest there is no overarching defect in the function of T_{CD8+} in the
240 absence of $\gamma\delta$ T cells.

241 To this point we have examined the recruitment, localization and function of bulk T_{CD8+}. It
242 was possible that the study of bulk T_{CD8+} of many specificities obscured subtle changes in some
243 antigen-specific T_{CD8+} populations. However, it was not possible to examine the function of
244 antigen-specific T_{CD8+} at the site of infection, as many cells had already been activated in the
245 presence of VACV-infected cells (**Fig.3E, F**). Therefore, we examined the antigen-specific
246 systemic T_{CD8+} response in the spleen 8d after dermal VACV infection of WT or TCR$\delta^{-/-}$ mice by
247 incubating splenocytes in the presence of 9 individual MHC Class I-binding peptides derived from
248 VACV. We measured production of IFN-γ and TNFα, each of which can exert antiviral effects and
249 which, when both produced by the same cells, indicate polyfunctionality that correlates with
250 protective capacity against virus infection [60]. The proportion of T_{CD8+} producing IFN-γ in
251 response to each epitope was greater than the proportion producing TNFα, but, across three
252 replicate experiments, there were no statistically significant differences in the responses observed
253 in WT and TCR$\delta^{-/-}$ mice. Taken together, these results indicate that $\gamma\delta$ T cells are unlikely to play
254 a significant role in the priming, recruitment, localization or subsequent function of T_{CD8+} in the
255 anti-VACV response. Therefore, T_{CD8+}-mediated immunopathology is unlikely to contribute to the
256 increased pathology we observe in VACV-infected TCR$\delta^{-/-}$ mice.
257

γδ T cells do not influence the local monocyte response to VACV.

It is possible that, rather than controlling immunopathology, γδ T cells coordinate the changes in the immune response that lead to resolution of inflammation and subsequent reduction of local tissue pathology. We have previously described a role for two recruited populations of monocytes in control of the severity of pathology observed following dermal VACV infection but these populations of monocytes do not have a large effect upon local VACV replication [11-13]. Both classical CD11b$^+$Ly6C$^+$Ly6G$^-$ monocytes and a population of CD11b$^+$Ly6C$^+$Ly6G$^+$ myeloid cells are recruited to the VACV lesion following i.d. infection [11, 12, 61]. The CD11b$^+$Ly6C$^+$Ly6G$^+$ myeloid cells are monocytic in nature and limit local tissue damage via production of reactive oxygen species [11]. In contrast, the classical CD11b$^+$Ly6C$^+$Ly6G$^-$ monocytes are attracted to the site of infection by Type I IFN-stimulated production of CCL4, and also moderate tissue damage, possibly by becoming infected and soaking up excess virions [13]. Since γδ T cells are found in the VACV lesion (**Fig. 1**), and are known to regulate myeloid cell activity after some insults [26, 27], we examined whether sensing of VACV by γδ T cells is required to moderate recruitment of either monocyte population. We harvested ears from infected WT or TCRδ$^{-/-}$ mice, and carefully gated monocyte populations to exclude innate lymphoid cells (ILCs), lymphocytes or resident or recruited dendritic cells (DC) (**Fig. 4A**). Five days after infection, a time point at which both virus replication and CD11b$^+$Ly6C$^+$Ly6G$^-$ classical monocyte infiltration peak, there was no difference in recruitment of either classical monocytes (**Fig. 4B, C**) or CD11b$^+$Ly6C$^+$Ly6G$^+$ myeloid cells (**Fig. 4B, E**) in VACV-infected WT compared to infected TCRδ$^{-/-}$ mice. Eight days after infection, when numbers of CD11b$^+$Ly6C$^+$Ly6G$^+$ myeloid cells peak, we also observed no difference in recruitment of either classical monocytes (**Fig. 4D**) or CD11b$^+$Ly6C$^+$Ly6G$^+$ myeloid cells (**Fig. 4F**) in VACV-infected WT compared to infected TCRδ$^{-/-}$ mice. In contrast to T_{CD8+}, both CD11b$^+$Ly6C$^+$Ly6G$^-$ monocytes and CD11b$^+$Ly6C$^+$Ly6G$^+$ myeloid cells enter the VACV lesion, where the CD11b$^+$Ly6C$^+$Ly6G$^-$ monocytes become infected, and CD11b$^+$Ly6C$^+$Ly6G$^+$ myeloid

283 cells produce ROS to moderate tissue damage [11, 59]. To examine whether γδ T cells control
284 the localization of each myeloid cell population, we infected WT or TCRδ$^{-/-}$ mice with VACV-GFP
285 and harvested on d7 post-infection, and then stained for either Ly6C or Ly6G. We observed similar
286 staining with Ly6C and Ly6G, both inside and outside of the GFP^{+} VACV lesion, in both WT or
287 TCRδ$^{-/-}$ mice. Therefore, our data indicate that γδ T cells do not play a requisite role in recruitment
288 or localization of three crucial components of local cellular antiviral immunity.
289
290 ***IFN-γ mediates pathology in VACV-infected skin***
291 Interferons are potent antiviral cytokines that are widely produced upon virus infection, but
292 which are also strongly linked to the pathology of many skin conditions, including psoriasis [62]
293 and alopecia areata [63]. We have demonstrated above that IFN-γ is produced by T_{CD8+} in
294 response to cutaneous VACV infection, but that this process is not affected by the absence of γδ
295 T cells (**Fig. 3 A-H**). However, direct production of IFN-γ by γδ T cells plays a role in control of
296 multiple viral infections [17-21], including poxviruses following systemic infection [8, 50, 51, 64].
297 Therefore, we examined the level of mRNA encoding IFN-γ in the VACV-infected ear at various
298 times after infection. We found a robust (~40-fold) and reproducible induction of *ifng* transcript by
299 3 days post-infection (**Fig. 5A**), a time point at which we have previously described there was little
300 to no immune cell infiltrate present [11]. The induction of *ifng* transcript continued to rise to ~1-
301 2000 fold within 7 days of infection, likely as a result of infiltration of activated T_{CD8+} and T_{CD4+}
302 (**Fig. 5A**).
303 To examine the functional consequence of production of IFN-γ following cutaneous VACV
304 infection, we measured the swelling of the VACV infected ear at early time points in WT vs. IFN-
305 γR$^{-/-}$ mice. We found that, as early as d3 post-infection, VACV-infected IFN-γR$^{-/-}$ mice displayed
306 increased swelling compared to WT mice (**Fig. 5B**). This correlated with development of a VACV
307 lesion 1d earlier in VACV-infected IFN-γR$^{-/-}$ vs. WT mice (**Fig. 5C-E**) and enhanced tissue loss at

later time points (**Fig. 5F-H**). IFN-γ is a potent antiviral cytokine that drives production of many interferon stimulated genes that act to control virus replication using a large variety of mechanisms. However, the increased local tissue pathology we observed was not a result of enhanced VACV replication in the absence of the antiviral action of IFN-γ, as WT and IFN-γR$^{-/-}$ mice displayed similar levels of replicating VACV in the ear at d5 post-infection (**Fig. 5I**). In addition, the absence of IFN-γ signaling did not alter spread of VACV from the ear, with similar low levels disseminating to spleen and ovaries by d5 post-infection (**Fig. 5 J,K**). Therefore, the phenotype we observe following VACV infection of IFN-γR$^{-/-}$ mice, namely a marked increase in tissue pathology compared to VACV-infected WT mice, without a corresponding increase in VACV replication of spread, closely mimics the phenotype we observed following VACV infection of TCRδ$^{-/-}$ mice.

To tease out the role of γδ T cell-mediated production of IFN-γ we examined the production of IFN-γ on d4 post-infection by staining for the intracellular cytokine, with or without activation of *ex vivo* isolated γδ T cell subsets by PMA/ionomycin. Somewhat surprisingly, *ex vivo* isolated γδ T cells of all kinds examined failed to stain for IFN-γ, even when activated with PMA-ionomycin for a number of hours before staining (**Fig. 5L**). As a control for our activation and staining, we examined IFN-γ production by T_{CD4+} and T_{CD8+} harvested from the lymph node of VACV infected mice on d4 post-infection, a time point prior to infiltration of these cell types to the site of infection (**Fig. 5M**). Although neither T_{CD4+} nor T_{CD8+} detectably produced IFN-γ in the absence of external stimuli, there was substantial and reproducible upregulation upon PMA/ionomycin stimulation (**Fig. 5M**), indicating that our assay was working.

Our observation that we could detect both *ifng* transcript (**Fig. 5A**) and an increase in swelling in IFN-γR$^{-/-}$ mice (**Fig. 5B**), but no detectable production of IFN-γ protein by cutaneous γδ T cells (**Fig. 5J**) at similar time points could potentially be explained by the relative insensitivity of the flow cytometry staining for IFN-γ protein. Therefore, we examined the levels of *ifng* transcript

in the ears of WT vs. TCR$\delta^{-/-}$ mice on d4 post-infection, the day on which we had previously conducted the flow cytometry analysis. As above, we found a marked induction of *ifng* transcript upon VACV infection of WT mice and this was enhanced slightly (~2-fold) in the absence of γδ T cells (**Fig. 5N**). Therefore, γδ T cells do not contribute to IFN-γ production upon cutaneous VACV infection, a marked departure from their role following systemic infection [8, 50, 51, 64].

Because γδ T cells are not required for IFN-γ production, and leukocytes are not recruited to the infected ear until after we began to observe induction of *ifng* transcript, we sought to identify the cell type producing IFN-γ early after dermal VACV infection. We infected mice, harvested cells from the ear on d4 post-infection and incubated them in the presence of Brefeldin A for 6h to prevent protein secretion, stained cells with cell-surface markers to identify cell types, and then intracellularly for IFN-γ. We divided cells in the ear into EpCAM^{-} CD45^{+} infiltrating immune cells, EpCAM^{+} CD45^{+} resident immune cell populations (which include resident γδ T cells) and EpCAM^{+} CD45^{-} keratinocytes (KC). As in all of our flow cytometry experiments, we used fluorescence minus one (FMO) controls, in which cells were stained with all antibodies except to IFN-γ, in order to distinguish our IFN-γ signal. We found that neither EpCAM^{-} CD45^{+} nor EpCAM^{+} CD45^{+} (including resident γδ T) cells stained for the presence of IFN-γ on d4 post-infection (**Fig. 5O, P**). However, somewhat surprisingly, a small proportion of EpCAM^{+} CD45^{-} KC, which comprise the majority of cells in the ear, did produce IFN-γ (**Fig. 5O, P**). Although the proportion of KC producing IFN-γ only increased from <0.1% of cells to ~0.54+/- 0.07 of cells, KC outnumber all resident and recruited cells in the skin >100:1, so this increase in the number of cells is very biologically significant.

γδ T cell subsets are responsible for IL-17 production in VACV-infected skin

After we had shown that γδ T cells did not produce IFN-γ after cutaneous VACV infection our attention turned to examine the production of other cytokines that have been implicated in

358 skin pathology. In particular, our attention turned to the γδ T cell-mediated production of IL-17A
359 for a number of reasons. First, there is a strict division between the production of IL-17A and
360 IFN-γ by γδ T cells [65], that may be controlled by the initiation of innate vs. adaptive signaling
361 within these cells [21]. Second, γδ T cells are the primary producers of IL-17 outside of gut tissue
362 [22, 23], including in cutaneous infection models. Vγ2$^+$ dermal γδ T cells are strong producers of
363 IL-17A following BCG infection [66] and Vγ3$^+$ DETCs produced IL-17A after cutaneous *S. aureus*
364 infection, [24, 25]. Third, γδ T cell-mediated production of IL-17A can also play a role in cutaneous
365 pathology, driving tissue damage in psoriasis [16, 67, 68] and dermatitis [69]. Fourth, γδ T cell-
366 mediated production of IL-17A can also play an important role in cutaneous wound healing [24].
367 Therefore, as γδ T cell-derived IL-17A clearly plays important roles in context-dependent anti-
368 pathogen, as well as tissue damaging and tissue protective responses, we examined the levels
369 of *il17a* mRNA transcript upon cutaneous VACV infection. There was a marked (~10-15-fold)
370 increase in *il17a* transcript in WT mice upon VACV infection (**Fig. 6A**). When we examined levels
371 of IL-17A protein produced in γδ TCR$^+$ or γδ TCR$^-$ cell populations by flow cytometry, using
372 approaches similar to those outlined above, we found that >80% of the cells producing IL-17A
373 were γδ T cells (**Fig. 6B**) early after infection. We further examined the ability of γδ T cell subsets
374 (Vγ3$^+$ DETC, Vγ2$^+$ dermal γδ T cells or Vγ3$^-$Vγ2$^-$ γδ T cells), to produce IL-17A directly *ex vivo*, or
375 whether they possessed the ability to produce IL-17A following activation with PMA/ionomycin.
376 A small proportion of both the Vγ2$^+$ dermal γδ T cells and Vγ3$^-$Vγ2$^-$ γδ T cells produced low
377 quantities of IL-17A directly *ex vivo* (**Fig. 6C, D**), and this production was enhanced by activation
378 with PMA-ionomycin (**Fig. 6C**). However, the Vγ3$^+$ DETC, which were the cells responding to
379 VACV infection by upregulating cytolytic activity, did not produce IL-17A (**Fig. 6C, D**), further
380 indicating functional specialization of γδ T cell subsets upon dermal VACV infection. To assess
381 the contribution of Vγ2$^+$ and Vγ3$^-$Vγ2$^-$ γδ T cells to the production of IL-17A following VACV
382 infection, we measured transcript levels of *il17a* mRNA in uninfected or infected WT or TCRδ$^{-/-}$

383 mice, 5 days after infection. The increase in *il17a* transcript in WT mice infected by VACV was
384 almost completely ablated in VACV-infected TCR$\delta^{-/-}$ mice (**Fig. 6E**), indicating that $\gamma\delta$ T cells,
385 directly or indirectly, are responsible for almost all IL-17A production upon virus infection.
386
387 ***Dermal VACV infection induces a response characteristic of wound healing***
388 Our data to this point indicated that both $\gamma\delta$ T cells and IFN-γ can have a profound impact
389 upon local tissue pathology following VACV infection, without a large effect upon local VACV
390 replication or systemic spread of the virus. This phenotype is reminiscent of those we have
391 observed in mice depleted of either of two different monocyte populations [11, 61], which lack
392 myeloid cell production of reactive oxygen species [11], or mice lacking Type I IFN signaling [13].
393 Therefore, we took a step back to examine the processes induced at the site of dermal infection
394 with VACV. We assessed the expression of various cytokines, chemokines, interferons, interferon
395 receptors and their signaling pathways in the skin of uninfected WT mice compared to VACV-
396 infected WT mice on d5 post-infection, a time point immediately prior to the development of
397 lesions and subsequent tissue loss. This analysis did not directly address the role of $\gamma\delta$ T cells,
398 as we only examined modulation of gene expression by VACV infection in WT mice, but it did
399 provide us with significant information with which to interrogate the role of $\gamma\delta$ T cells (see below).
400 In total, our gene profiling examined the expression of 160 unique transcripts 72 of which (45%)
401 were statistically changed more than 2-fold (50 upregulated, 22 downregulated) upon VACV
402 infection (**Fig. 7A**) Our focused approach allowed us to identify that ~76-77% of the 50
403 upregulated and 22 downregulated transcripts had a defined role in the process of cutaneous
404 wound healing (upregulated wound healing genes in red and downregulated wound healing genes
405 in blue in **Fig. 7A**) [70-72], producing a putative gene signature for a virus induced-wound healing
406 response in skin, shortly after infection.

Of the transcripts that were modulated by VACV infection, and have a role in cutaneous wound healing, were CC chemokines (**Fig. 7B**) and CXC chemokines (not shown), which function to recruit innate and adaptive immune effector cells, and all of which were upregulated. There were also marked upregulations of IL-10 superfamily members, including *il10*, *il22* and *il24* (which was upregulated ~400-fold), and downregulation of the antagonist of the IL-10 superfamily member IL-20, *il20ra* (**Fig. 7C**). Transcripts for other cytokines with a positive role in wound healing, such as *il1b*, *il6* and *il9*, were upregulated, while cytokines that have an inhibitory role in wound healing, such as *il16* and *il4*ra, were downregulated upon VACV infection (**Fig. 7D**).

Growth factors such as vascular endothelial growth factor (*vegf*), Leukemia inhibitory factor (*lif*), and osteopontin (*spp1*) were also upregulated by VACV infection (**Fig. 7E**). Somewhat surprisingly, transcripts of receptors for a number of growth factors involved in wound healing, including the growth hormone (*ghr*), leptin (*lepr*) and erythropoeitin (*epor*) receptors, were downregulated in response to VACV infection, along with the hormones thrombopoietin (*thpo*) and adiponectin (*adipoq*) (**Fig. 7A**). This indicates that the presence of VACV infection in the skin may modulate the classical wound healing response, creating a unique poxvirus/wound healing signature. In addition, members of the Transforming Growth Factor-β superfamily (*tgfb2*, *bmp2*, *bmp4* and *bmp6*) that play a role in fibrosis and scar formation in the classical wound healing response [73, 74], were also downregulated upon VACV infection (**Fig. 7F**), further indicating a departure from the classical response.

γδ T cells modulate expression of genes involved in wound healing after VACV infection.

We expanded on our findings to examine the impact of a constitutive deficiency in γδ T cells upon the expression of cytokines and chemokines identified above as being involved in the wound healing process initiated by dermal VACV infection. As above, we utilized qPCR arrays to profile gene expression of day 5 post-infection. Importantly, in order to rule out any contribution

of constitutive changes in gene expression in TCR$\delta^{-/-}$ mice, we initially analyzed gene expression in these mice compared to WT mice, in the absence of infection. We found that a number of transcripts were upregulated in uninfected mice in the absence of $\gamma\delta$ T cells, including *cxcl13*, *il23a* and *il12b* (**Fig. 8A**). We also found that *adipoq* and *il16*, which are genes involved in wound healing that we have previously shown to be modulated during VACV infection, were constitutively downregulated in the skin of TCR$\delta^{-/-}$ mice, implying that a constitutive alteration in wound healing may exist in these mice (**Fig. 8A**). However, as we observed a change in *adipoq* and *il16* in the absence of infection in TCR$\delta^{-/-}$ mice, we could not draw any conclusions about the role of these genes in the response after VACV infection. We next examined changes in gene expression in uninfected vs. infected TCR$\delta^{-/-}$ mice to reveal VACV-induced changes in gene expression in these mice. We found a similar pattern of gene expression changes to that shown in Fig. 7A, with both upregulation and downregulation of numerous cytokines and chemokines, some of which are involved in wound healing (upregulated wound healing genes in red and downregulated wound healing genes in blue in **Fig. 8B**). Therefore, to examine the contribution of $\gamma\delta$ T cells to gene expression exclusively after VACV infection, we compared gene expression in WT vs TCR$\delta^{-/-}$ mice 5 days after dermal VACV infection, a time point at which there is no significant difference in titers of VACV within the infected ear (**Fig. 2D**). We found that a number of transcripts are induced to higher levels in TCR$\delta^{-/-}$ mice than WT mice, including a number of interferon-responsive chemokines such as *cxcl9*, *cxcl13* and *ccl5* (**Fig. 8C**). This correlates with enhanced expression of *ifna2* observed in VACV-infected TCR$\delta^{-/-}$ mice (**Fig. 8B**). However, we also observed that two IL-10 superfamily members, *il10* and *il22*, which were upregulated upon dermal VACV infection (**Fig. 7A**), were not upregulated in VACV-infected TCR$\delta^{-/-}$ mice (**Fig. 8B**), and were markedly (8-15 fold) and significantly downregulated in VACV-infected TCR$\delta^{-/-}$ mice vs. VACV-infected WT mice (**Fig. 8C**). Notably, expression of neither *il10* nor *il22* was modulated in

456 uninfected TCR$\delta^{-/-}$ mice (**Fig. 8A**), indicating that the deficiency in *il10* and *il22* expression was
457 both $\gamma\delta$ T cell- and VACV-dependent.

458 To examine whether $\gamma\delta$ T cells express IL-22 directly, or cause it's production indirectly,
459 we utilized Catch22 mice, in which the IL-22 promoter drives expression of the fluorescent
460 reporter molecule, tdTomato [75]. We infected those mice i.d. with VACV expressing GFP,
461 harvested cells on d5 post-infection and assessed tdTomato fluorescence in GFP$^+$ and GFP$^-$ cell
462 populations liberated from the ear. As expected, and as previously published [59] we found that
463 a large number (~7%) of EpCAM$^+$CD45$^-$ KCs were VACV-infected, but we found no tdTomato
464 fluorescence in either infected or uninfected KC populations (**Fig. 8D**). We next separated
465 immune cell populations present at the site of VACV infection into resident (EpCAM$^+$CD45$^+$, **Fig.**
466 **8E**) or recruited (EpCAM$^-$CD45$^+$, **Fig. 8G**) populations. Both resident and recruited populations
467 displayed significant levels of infection (GFP fluorescence, **Fig. 8E, G**), but the resident population
468 displayed a much higher proportion of cells displaying IL-22 production than the much more
469 numerous recruited population (tdTomato fluorescence, **Fig. 8E, G**). Within the resident immune
470 cells, there were distinct populations of cells that were infected (GFP$^+$), infected and producing
471 IL-22 (GFP$^+$ tdTomato$^+$), and uninfected but also producing IL-22 (GFP$^-$ tdTomato$^+$) (**Fig. 8E**). To
472 ascertain the contribution of resident $\gamma\delta$ T cells to IL-22 production, we also stained cells with an
473 anti-$\gamma\delta$ TCR antibody. We were able to observe VACV infection of resident EpCAM$^+$ $\gamma\delta$ T cells
474 (**Fig. 8F**), as previously (**Fig. 1C**), and a large population of IL-22-producing resident $\gamma\delta$ T cells
475 (**Fig. 8F**), but production of IL-22 by VACV-infected $\gamma\delta$ T cells was minimal (**Fig. 8F**). Therefore,
476 it is likely that other resident CD45$^+$ cells that are VACV-infected also contribute to production of
477 IL-22. Within the recruited (EpCAM$^-$) immune cell populations, IL-22 production has often been
478 attributed to a population of T_{CD4+}, so we examined VACV infection and IL-22 production in $\gamma\delta$
479 TCR$^-$ lymphocyte populations (**Fig. 8H**) and compared this to infection of, and IL-22 production
480 by, recruited $\gamma\delta$ T cells (**Fig. 8I**). We found that infection of both populations of recruited

lymphocytes was minimal (**Fig. 8H, I**), but that recruited γδ T cells, and not other lymphocytes, also produced IL-22. Finally, we examined the contribution of γδ T cells to *il22* mRNA levels on d5 post-VACV infection of the ear, and found that, although there was a slight increase in *il22* transcript levels in VACV-infected TCRδ$^{-/-}$ mice compared to uninfected TCRδ$^{-/-}$ mice, this induction was markedly and statistically significantly lower than the induction we observed in VACV-infected WT mice (**Fig. 8J**). Taken together, the data from **Figure 8 D-J** indicate that both resident and recruited γδ T cells are major producers of IL-22 during dermal VACV infection.

To examine whether γδ T cells express IL-10, the other molecule we identified as modulated in the VACV-infected ear, we utilized mice in which an internal ribosome entry site (IRES)-enhanced green fluorescent protein (*eGFP*) fusion protein was placed downstream of exon 5 of the interleukin 10 (*Il10*) gene (Vert-X mice) [76]. We were able to detect a small but distinct and reproducible population of cells liberated from the VACV-infected ear that were GFP^{+} 5d after infection of the IL-10-GFP reporter mice (**Fig. 8L**), but not of WT mice (**Fig. 8K**). CD45^{-} EpCAM^{+} KCs did not contribute to the IL-10-GFP signal observed (not shown), and the d5 time point examined is prior to accumulation of antigen-specific T_{CD8+} [11, 61] that have been shown to produce IL-10 [77], so we examined IL-10 production by resident (EpCAM^{+}) or recruited (EpCAM^{-}) γδ T cells or myeloid cells, as previously identified in **Figure 4**. In contrast to the γδ T cell production of IL-22 observed above (**Fig. 8F**, **I**), we did not find IL-10 production by either resident or recruited γδ T cell populations (**Fig. 8M**, **O**). In contrast, we did find production of IL-10/GFP by resident, but not recruited, myeloid cells populations (**Fig. 8N**, **P**). Therefore, γδ T cells do not appear to express IL-10 directly upon VACV infection, but may modulate it's expression in other ways.

Our identification of γδ T cell-modulated genes above is a minimalistic one, so we sought to examine a number of other genes that have been linked to both γδ T cells and wound healing. Two of these genes, Fibroblast growth factor 9 (*fgf9*, **Fig. 8Q** [39]) and Keratinocyte Growth Factor

506 (*fgf7*, **Fig. 8R** [41]) were upregulated in the ear >40-fold at d5 post-VACV infection in WT mice,
507 but *fgf9* was not upregulated above the levels observed in uninfected mice in VACV-infected
508 TCR$\delta^{-/-}$ mice (**Fig. 8Q**), and the upregulation of *fgf7* was markedly reduced (**Fig. 8R**). Therefore,
509 $\gamma\delta$ T cells directly or indirectly modulate the expression of multiple genes involved in the wound
510 healing program initiated by cutaneous VACV infection.

Discussion

It is generally accepted that the local innate immune response to a peripheral virus infection is designed to slow virus replication and spread until an adaptive response can be initiated that will eliminate the virus and prevent re-infection. However, a key factor governing the extent of both the innate and adaptive immune response is that neither response should deleteriously affect the host, making it more susceptible to secondary infections, particularly via loss of barrier functions in the periphery (skin, airways etc.). Typically, this is represented in textbooks as a temporally regulated process, with the immune system gaining control over the virus, followed by a subsequent switch to reparative mechanisms that ameliorate tissue damage inflicted by both the virus and the ensuing host response. However, in this report we have described the initiation of a wound healing program in the skin concurrent with the deployment of innate antiviral strategies. The action of this wound healing program can alter tissue pathology following virus infection, independent of the control of virus replication and spread. The presence of two ongoing responses at the same time, and in very close physical proximity to each other, raises the possibility that the antiviral and wound healing responses could act synergistically to enhance each other by increasing the efficiency of monocyte recruitment, or interferon production (see below). However, it is also possible that components of one response will act to decrease the efficiency of the other. In either case, it is clear that wound healing after a cutaneous virus infection differs mechanistically from sterile wound healing, creating novel points of therapeutic intervention that could enhance wound healing and successful closure of the barrier surface to prevent secondary bacterial infection.

In a number of previous manuscripts we and others have described a role for various aspects of the local innate immune response, including two distinct monocyte populations [11, 59], reactive oxygen species [11] and Type I IFN [13], in amelioration of tissue damage following peripheral VACV infection. However, in each of these publications we found little or no effect of these components of the innate immune response upon local virus replication, despite often

538 profound effects upon local tissue pathology [11, 13, 59]. Having outlined a wound healing
539 program initiated upon cutaneous virus infection here, we can now retrospectively place each of
540 these innate immune responses into that program. Recruitment of monocytes to a wound is
541 required for effective wound healing to occur [78, 79], as is the Type I IFN receptor [80, 81].
542 Similarly, Ly6G$^+$ cells are recruited to a wound [82]) and produce nitric oxide to facilitate
543 accelerated wound healing [83]. Following VACV infection Ly6G$^+$ cells produce ROS, which can
544 also act to increase wound healing [84], and ablation of ROS production following VACV infection
545 causes a large increase in pathology [11]. Therefore, all of our previous observations in which
546 depletion or ablation of various components of the immune system has minor changes upon local
547 virus replication, but substantial changes upon local tissue pathology, can be attributed to
548 alterations in an early wound healing response.

549 Here, we initially investigated the role of γδ T cells in control of replication and spread of
550 VACV following cutaneous infection. γδ T cells have been implicated in the host response to VACV
551 [7-10] and other poxviruses [49-53] after systemic infection. This protective effect has been
552 attributed to cytolytic activity against VACV-infected cells [7, 10], or to γδ T cell-mediated
553 production of IFN-γ [8, 50]. Here, following cutaneous infection with VACV, we show that
554 epidermal Vγ3$^+$ DETC, which are a major population in mice but not in humans [85], acquire a
555 GzB$^+$ CD107a$^+$ cytolytic phenotype. Neither the resident nor recruited dermal γδ T cell populations
556 acquire this cytolytic phenotype. However, we and others [86] have found no difference in VACV
557 replication in the skin of mice lacking γδ T cells, so any cytolytic contribution of these cells may
558 be compensated for by infiltrating αβ T cells. None of the resident or recruited cutaneous γδ T cell
559 populations appeared to be primed to make IFN-γ after VACV infection, even after *in vitro*
560 restimulation, and there was a small increase in IFN-γ production in the skin of VACV-infected
561 TCRδ$^{-/-}$ mice compared to WT mice. However, KCs did make IFN-γ protein shortly after VACV
562 infection, and this contributed to control of pathology, but not to control of VACV replication.

563 Therefore, the functions previously attributed to γδ T cells in control of virus replication and virus-
564 induced pathology do not play a role in the pathology observed after cutaneous infection of TCRδ$^{-/-}$
565 mice with VACV.

566 A sizeable portion of dermal γδ T cells produced IL-17A after cutaneous VACV infection,
567 a cytokine that is required for efficient wound healing [24, 87]. IL-17A mRNA was reduced to
568 almost background levels in VACV-infected TCRδ$^{-/-}$ mice 5 days after infection, a time point that
569 precedes the later infiltration of T_{CD4+} that may produce IL-17A. Indeed, 8 days after infection, it
570 was primarily T_{CD8+}, not T_{CD4+}, that produced IL-17A upon the restimulation of αβ T cells from
571 infected skin. However, at early time points after infection, dermal γδ T cells likely moderate wound
572 healing, at least partially, via production of IL-17A in response to cutaneous VACV infection. γδ T
573 cells have long been known to play a role in cutaneous wound healing after activation by KCs
574 [30-33], where they migrate to a site of injury [26, 34, 35] and produce of a number of cytokines
575 that promote the wound healing response [36-44]. We did find a marked increase in VACV-
576 induced pathology in the absence of γδ T cells, consistent with a role for these cells in
577 establishment of the wound healing response following VACV infection.

578 Our data clearly demonstrate that γδ T cells are modulating VACV-induced skin
579 pathology. The enhanced wound that results from VACV infection in the absence of γδ T cells
580 prompted us to examine the range of wound healing-associated molecules induced by VACV
581 infection that is discussed above. When we examined changes in the wound healing signature
582 induced by cutaneous VACV infection in TCRδ$^{-/-}$ mice we originally anticipated that γδ T cells may
583 alter the profile of chemokines that are induced. This is because γδ T cells have previously been
584 reported to change recruitment of monocytes and neutrophils [26, 27], including after VACV
585 infection [86]. In addition, IL-17A is reported to modulate neutrophil recruitment via an effect on
586 expression of CXC chemokines [88], so in the absence of γδ T cell-produced IL-17A a defect in
587 neutrophil recruitment would be anticipated. However, we found no discernable role for γδ T cells

588 in modulation of chemokine or chemokine receptor expression after VACV infection, and
589 observed equivalent recruitment of myeloid cell populations in VACV-infected WT and TCR$\delta^{-/-}$
590 mice. The differences we observed from a previously published report, in which VACV-infected
591 TCR$\delta^{-/-}$ mice exhibited less pathology than infected WT mice, likely because of alterations in
592 neutrophil recruitment [86], may be attributable to the cutaneous microbiome in animal facilities.
593 We have anecdotally observed a marked difference in both the magnitude and mechanisms
594 involved in VACV-induced pathology in mice in the presence or absence of pathogenic bacteria,
595 so strive to ensure that mice are kept as pathogen-free as possible without rederivation into a
596 germ-free facility. The composition of the skin microbiome has a profound effect upon wound
597 healing [89], and future studies in germ-free animals reconstituted with different skin-resident
598 bacteria will likely reveal roles for specific bacterial/host interactions after both “sterile” and virus-
599 infected wounding.

600 When we examined the difference between the constitutive expression of wound healing-
601 associated cytokines in WT vs TCR$\delta^{-/-}$ mice we found two genes that were downregulated in
602 TCR$\delta^{-/-}$ mice, in the absence of virus infection. Expression of these two genes that encode IL-16
603 and adiponectin was also reduced in infected TCR$\delta^{-/-}$ mice vs. infected WT mice. IL-16 typically
604 increases inflammation in the skin and inhibits the wound healing response [90], but adiponectin
605 promotes wound healing by increasing KC proliferation and migration [91]. Therefore, deficits in
606 $\gamma\delta$ T cells may partially account for the previously described defect in sterile wound healing [32,
607 44] via reduced expression of adiponectin.

608 Upon VACV infection of TCR$\delta^{-/-}$ mice, we found a similar response to that observed in WT
609 mice, with upregulation of many of the mediators of wound healing that we had observed in WT
610 mice, and downregulation of a similar pattern of cytokines as well. However, there were two
611 marked changes between VACV-infected TCR$\delta^{-/-}$ and WT mice, namely a failure to upregulate
612 expression of the IL-10 family members, *il22* and *il10*, in TCR$\delta^{-/-}$ mice in response to VACV

infection. IL-10 is produced after VACV infection by T_{CD8+}, but is also induced prior to the infiltration of large numbers of these cells, indicating a role for γδ T cell-mediated production. However, although γδ T cells from the liver can produce IL-10 following bacterial infection [92], we found that γδ T cells do not produce IL-10 themselves, but induce production from other cells, likely skin-resident myeloid cells such as Langerhans cells and dermal DC (**Fig. 8 M, N, O**). IL-10 production drives skin regeneration, likely by altering the phenotype of macrophages, as the IL-10R is not expressed by KCs [93]. Therefore, a reduction in IL-10 expression may drive part of the increase in pathology we observe following VACV infection of TCRδ$^{-/-}$ mice. Such an increase in pathology may actually be detrimental to the virus, as some skin-tropic poxviruses encode an IL-10 homolog that enhances wound healing [94-97], indicating that IL-10 expression may be evolutionarily beneficial for the virus during natural skin infection, perhaps by inhibiting the chances of a competing local secondary bacterial infection.

Expression of IL-22 is often associated with inflammatory skin conditions, such as psoriasis [98], where it is often co-expressed with IL-17A [99]. Expression of both IL-22 and IL-17A are most often associated with Th17 T_{CD4+} cells, but both cytokines are produced in large quantities in cutaneous tissue by γδ T cells [100]. Although technical issues prevented us from establishing that the same populations of γδ T cells produce both IL-17A and IL-22 following cutaneous VACV infection, it is clear that the majority of these cytokines produced at d5 post-VACV infection come from γδ T cells, and these cytokines likely drive important components of the early wound healing response. IL-22 acts on dermal fibroblasts to drive expression of extracellular matrix proteins [101], and on KCs to increase proliferation [98, 102, 103] via miR-197-driven mechanisms [104], as observed after bacterial skin infection [105]. In addition to the IL-10 family members, we also found that expression of both *fgf7* (encoding KC Growth factor) and *fgf9* were markedly reduced in VACV-infected TCRδ$^{-/-}$ mice, consistent with reports of their

637 production by γδ T cells and roles in cutaneous wound healing [39, 44]. Therefore, γδ T cells
638 contribute in multiple ways to the cutaneous wound healing response following VACV infection.
639 In summary, we find here that neither resident nor recruited γδ T cells, nor cytokines
640 produced by these cells, are involved in control of virus replication or spread following cutaneous
641 infection. Rather, we describe here a uniquely configured wound healing response initiated in the
642 skin of virus-infected mice prior to the peak of virus replication and before adaptive immune
643 mechanisms have been deployed successfully to clear the infection. We find that both resident
644 and recruited γδ T cells are part of this induced wound healing response via production of IL-17A,
645 IL-22 and induction of IL-10 in other cells, and that a deficit in γδ T cells causes a profound
646 increase in tissue pathology following infection. These findings are important in understanding
647 how wound healing is mediated following a cutaneous virus infection in comparison to the
648 paradigm of sterile wound healing. A prompt and appropriately controlled wound healing response
649 is crucial to prevent secondary bacterial infections that could be deleterious for the virus-infected
650 host, but also potentially for the virus itself.

Materials and Methods

Mice

C57BL/6 (wild-type, WT) mice were purchased from Charles River Laboratories or Jackson Laboratories. Breeding pairs of B6.129P2-Tcrd^{tm1Mom}/J (TCR$\delta^{-/-}$) [106], IL-10/GFP (Vert-X) reporter mice [76], and IL-22/tdTomato (Catch22) reporter mice [75] were purchased from Jackson Laboratories. These mice were on a WT background after a minimum of 12 backcrosses to C57BL/6 and bred in the specific-pathogen-free animal facility at the Penn State Hershey College of Medicine. All animals were housed and cared for according to guidelines from the National Institutes of Health and American Association of Laboratory Animal Care (AALAC). The Penn State Hershey College of Medicine Institutional Animal Care and Use Committee (IACUC) approved all animal experiments and procedures.

Viruses and infections

Stocks of VACV strain WR were produced in 143B TK$^-$ cells and purified from cell lysate following ultracentrifugation through a cushion of 45% sucrose. VACV-GFP was previously described [107]. For intradermal (i.d.) infections, mice aged 7-10 weeks were anesthetized with ketamine/xylazine and injected with 10^4 PFU of VACV in <10 µL in each ear pinna.

To monitor pathogenesis in the ears, ear thickness was measured using a 0.0001 in. micrometer (Mitutoyo, Aurora, IL). Lesion progression and subsequent tissue loss were subsequently measured daily. To measure titers of virus *in vivo,* ears and ovaries (the target organ of VACV systemic spread [12]) were freeze-thawed three times, homogenized, and sonicated, then titers in cell lysates were assayed by plaque assay on 143B TK$^-$ cells as previously described [61]. Plaques were counted two days later.

Cell isolation and flow cytometry

Pairs of ears from each mouse were split into dorsal and ventral halves, minced, and digested in a solution of 1 mg/mL collagenase type XI (Sigma-Aldrich, St. Louis, MO) in media supplemented with 2% FBS and 5 mM $CaCl_2$ for 1 hour at 37°C, 5% CO_2. Collagenase was quenched with media containing 5% FBS and 5 mM EDTA. Digested tissue was passed through 40 μm nylon cell strainers to create a single cell suspension. For intracellular cytokine staining and CD107a degranulation assays, cells from 3 pairs of ears were pooled and 10^6 of those cells stimulated prior to staining for flow cytometry (see below).

Blockade of FcR-mediated binding of mAbs and subsequent staining of cells was performed in supernatant from flasks of 2.4G2 hybridoma cells supplemented with 10% normal mouse serum. All mAbs used were purchased from BD Pharmingen: CD45 (30-F11), CD3ε (145-2C11), TCRδ (GL3), CD4 (RM4-5), NK1.1 (PK136), CD19 (1D3), CD90.2 (53-2.1), CD11b (M1/70), Ly6C (AL-21), Ly6G (1A8), CD107a (1D4B), Granzyme B (GB11), IL-17A (TC11-18H10), TNFα (MP6-XT22) and IFN-γ (XMG1.2). We also utilized the following from Biolegend: Vγ2 TCR (UC3-10A6), Vγ3 TCR (536) and CD64 (X54-5/7.1). CD8α (53-6.7) and CD11c (N418) were obtained from eBioscience. In addition, PE-Cy7 conjugated streptavidin (eBioscience) was used to label biotin-conjugated antibodies. To stain for granzyme B, cells were stained for surface markers, fixed in 2% paraformaldehyde (Electron Microscopy Sciences, Hatfield, PA), then permeabilized and stained intracellularly for granzyme B in 2.4G2 supernatant containing 10% normal mouse serum and 0.5% saponin (Sigma). Sample data was acquired on either an LSR II or LSR Fortessa flow cytometer (both from BD Biosciences, San Jose, CA) and analyzed using FlowJo software (Tree Star, Ashland OR).

Intracellular cytokine staining assay

Single cell suspensions of ears were stimulated for 5 hours at 37°C, 5% CO_2 with 50 ng/mL phorbol myristate acetate (PMA; Sigma) and 1 μg/mL ionomycin (Sigma) or unstimulated in the

presence of 10 µg/mL brefeldin A (BFA; Sigma). For T cell stimulations, lymphocytes were isolated by centrifugation over Lymphocyte Separation Medium (Cambrex) and then stimulated for 4 h with 1 µM VACV peptide prior to the addition of BFA. VACV-derived peptides B8R, A8R, A3L, A23R, K3L, A47L, A42R, A19L, 10G2 have been previously described [108]. Following PMA/ionomycin or peptide stimulation, cells were blocked in 2.4G2 supernatant containing 10% mouse normal mouse serum and then stained for CD45, CD3ε, TCR δ, Vγ2 TCR, Vγ3 TCR, and CD4. Cells were fixed in 2% paraformaldehyde then permeabilized and stained for intracellular IL-17A and IFN-γ in 2.4G2 supernatant supplemented with 10% normal mouse serum and 0.5% saponin. Net frequencies and numbers of cytokine-positive T_{CD8+} were calculated by subtracting the unstimulated background response.

CD107a degranulation assay

Cells from ears were stimulated for 5 hours at 37°C, 5% CO_2 with 50 ng/mL PMA and 1 µg/mL ionomycin or unstimulated in the presence of 1.5 µg/mL monensin (Sigma) and PE-conjugated rat anti-mouse CD107a. Following stimulation, cells were blocked in 2.4G2 supernatant containing 10% normal mouse serum and then stained for CD45, CD3ε, TCR δ, Vγ2 TCR, Vγ3 TCR, and CD8α.

Immunofluorescence Microscopy

Ears were harvested and embedded in Tissue-Tek OCT (Sakura Finetek), then rapidly frozen by immersion in liquid nitrogen-cooled 2-methyl butane, and kept at -80 °C overnight. Cryostat sections (10-12 µm) were cut at -20°C, mounted on glass slides, air-dried for 2-3 hours, fixed for 10-15 minutes in 1% paraformaldehyde (pH 7.4), air-dried again for 30 minutes, and stained with antibodies to TCRδ , Ly6C, Ly6G or CD8 (clones as above). Positive signal was revealed by subsequent staining with fluorescently-labeled secondary antibodies. Staining was

visualized using an Olympus 1X81 deconvolution microscope and Slidebook 5.0 digital microscope.

Quantitative PCR

Tissues were harvested, digested as above, and total RNAs were extracted using RNeasy Plus Mini Kit (Qiagen) with DNase treatment according to the manufacturer's protocol. For qPCR using Taqman Gene Expression Assays (Applied Biosystems) or Universal Probe Library (Roche), cDNA was prepared using the Hi-Capacity cDNA Synthesis Kit (Applied Biosystems). For qPCR using RT^2 PCR Profiler Arrays (Qiagen), cDNA was prepared using RT^2 First Strand Kit (Qiagen). qPCR was carried out on a StepOnePlus (Applied Biosystems) with either FastStart Universal Probe Master Mix (Roche) or RT^2 SYBR Green qPCR Master Mix (Qiagen). For Taqman and FastStart Universal Probe assays, changes in gene expression are expressed as fold change using the $\Delta\Delta^{Ct}$ calculation method against naïve mice of the same genotype with *gapdh* as the housekeeping gene. For RT^2 PCR Profiler Array data, changes in gene expression are displayed as mean fold change between groups of mice relative to a panel of "housekeeping" genes. SYBR Green primers were as follows: *fgf7* forward 5′-ATAGAAACAGGTCGTGACAAGG-3′ reverse 5′-CAGACAGCAGACACGGAAC-3′
fgf9 forward 5′-GTAGAGTCCACTGTCCACAC-3′ reverse 5 ′-CAACGGTACTATCCAGGGAAC-3′. Taqman primer/probe sets (Thermo Fisher) were as follows: *il17a* (Mm00439618_m1), *il22* (Mm00444241_m1), *gapdh* (Mm99999915_gl) and *ifng* (Mm01168134_m1).

Acknowledgements

We thank colleagues Drs. Jon Yewdell and Jack Bennink for the WR VACV used in these studies. We thank Melanie Epler and Jennifer Mellinger for excellent technical support of these studies. We also the Penn State College of Medicine flow cytometry core facility and Karen Briar, Robin Goshorn, Jeanette Mohl, Dr. Tim Cooper, and Dr. Tiffany Whitcomb for essential animal handling and veterinary assistance. We also thank Dr. Nick Buchkovich for critical review of the manuscript.

Author Contributions

Conceived and designed the experiments: IER, EL, AMN and CCN. Performed experiments: CCN, EL, IER, TEK, and NJP. Analyzed the data: EL, IER, TEK, and NJP. Wrote the paper: CCN.

761 **Figure Legends**

762 **Figure 1. Infected and uninfected γδ T cells localize within VACV-infected foci in the skin.**
763 WT (**A**) and TCRδ$^{-/-}$ (**B**) mice were infected with 10^4 PFU of VACV-GFP using a bifurcated needle.
764 At d4 p.i., ears were harvested, frozen and sections stained with antibody to TCRδ (red). Infected
765 GFP+ cells are visualized in green. (**C**) To confirm that VACV infected γδ T cells, we infected mice
766 i.d. with 10^4 PFU of VACV, or VACV-GFP, then harvested and digested ears for flow cytometric
767 analysis on d4 p.i.. A proportion of γδ T cells, identified as CD45$^+$, CD3$^+$, γδ TCR$^+$ showed clear
768 GFP fluorescence. (**D**) For all subsequent analyses, debris and dead cells were first excluded by
769 a "live" cell gate. Singlets were identified by side scatter area (SSC-A) vs forward scatter width
770 (FSC-W), and then lymphocytes gated according to light scatter area. Within CD45$^+$ cells, CD3ε$^+$
771 T cells were subdivided into γδ T cells (TCRδ$^+$) and αβ T cells (TCR δ$^-$), which include T_{CD4+} and
772 T_{CD8+}. γδ T cell subsets in the skin were identified as follows: Vγ3$^+$ dendritic epidermal T cells
773 (DETC) and Vγ2$^+$ or Vγ2$^-$Vγ3$^-$ dermal γδ T cells. Data depicts T cells in ears of WT mice at d4 p.i.
774 with VACV and is representative. (**E**, **F**) WT mice were infected i.d. with 10^4 pfu VACV. Cells were
775 harvested from whole ears of mice at d0 (uninfected), 2, 4, 8, 10, 15, and 25 p.i. and T cell
776 responses monitored by flow cytometry. (**E**) Numbers of total γδ T cells (CD3ε$^+$TCRδ$^+$, black
777 circles), T_{CD4+} (CD3ε$^+$TCRδ$^-$CD4$^+$, gray squares), and T_{CD8+} (CD3ε$^+$TCRδ$^-$CD8α$^+$, triangles) cells
778 per pair of uninfected and infected ears. (**F**) Numbers of epidermal-resident Vγ3$^+$ DETC (gray
779 circles) compared to Vγ2$^+$ or Vγ2$^-$Vγ3$^-$ dermal γδ T cells (black squares and diamonds,
780 respectively) in ears after i.d. VACV infection. Values at each time point represent the mean ±
781 SEM in 6-10 pairs of ears from 3 independent experiments.
782
783 **Figure 2. Infected TCRδ$^{-/-}$ mice display enhanced tissue pathology, but no difference in**
784 **local VACV replication or systemic virus spread.** WT (**A**-**F**, **E**, **I**, **H**, **K**) or TCRδ$^{-/-}$ (**C**-**E**, **G**, **H**,
785 **J**, **K**) mice were infected i.d. in the ear pinnae with 10^4 pfu of VACV and ears harvested and

dissociated for analysis on d4 (**A**, **B**) or d8 (as shown, **A**, **B**) post-infection. Gating strategies are as shown in Figure 1. Potential cytolytic function, was measured by cell surface expression of CD107a (LAMP1) in response to activation with PMA-ionomycin (**A**), or intracellular expression of granzyme B (**B**) by $V\gamma3^+$ DETC, $V\gamma2^+$ or $V\gamma2^-V\gamma3^-$ dermal γδ T cells, T_{CD4+} or T_{CD8+} on d4 or d8 post-infection. T_{CD8+} were undetectable at the site of infection at d4 post-infection, so are only shown at d8 post-infection. (**C**-**E**, **H**, **K**) WT (circles) or TCRδ $^{-/-}$ (squares) mice were infected i.d. in the ear pinnae with 10^4 PFU of VACV. On d5 (**C**) and d12 (**D**) p.i., pairs of ears and ovaries were harvested from infected WT and TCR$\delta^{-/-}$ mice to measure titers of VACV by plaque assay. Data is representative of 7 pairs of ovaries and ears per group from 2 independent experiments. Tissue swelling (**E**) was assessed through 6 days after infection. The appearance of lesions in WT (**F**) or TCR$\delta^{-/-}$ (**G**) mice was visualized 8 days after infection, and lesion size quantified (**H**) through 21 days post infection. The ensuing tissue loss in WT (**I**) or TCR$\delta^{-/-}$ (**J**) mice was visualized 14 days after infection and quantified (**K**) through 21 days post infection. Data in (**E**, **H** and **K**) depict the mean ± SEM of 30 ears per group from 3 independent experiments. *p<0.05, **p<0.005, ***p<0.0001 by Student's t-test.

Figure 3. T_{CD8+} recruitment, localization and function are not affected in the absence of γδ T cells. WT or TCR$\delta^{-/-}$ mice were infected i.d. with 10^4 PFU VACV per ear and cells harvested to analyze the recruitment, localization and function of T_{CD8+}. Ears were harvested on d5 (**A**) or d8 post infection (**B**-**H**) and numbers of T_{CD8+} (**A**, **B**), localization of T_{CD8+} (in red) relative to VACV infected cells (in green) (**C**, **D**), numbers of T_{CD8+} in the VACV infected ear producing IFN-γ (**E**) or TNFα (**F**) directly ex vivo or proportion of splenic T_{CD8+} producing IFN-γ (**G**) or TNFα (**H**) in response to stimulation with VACV-derived MHC Class I binding epitopes.

Figure 4. Monocyte recruitment and localization is normal in mice lacking γδ T cells. WT and TCRδ$^{-/-}$ mice were infected i.d. in each ear pinnae with VACV. Gating strategy is shown in **A**. As in Figure 1, we first excluded debris and dead cells by scatter area and then gated on singlets by scatter area vs width. B cells, T cells, non-NK innate lymphoid cells (ILCs), and NK cells were "dumped" from CD45^{+} cells by excluding CD19^{+}, CD90.2^{+} and NK1.1^{+} cells. CD45^{+}CD19^{-}CD90.2^{-} NK1.1^{-}CD11c^{-}CD11b^{+} monocyte/macrophages were subdivided into Ly6C^{+}Ly6G^{-} classical inflammatory monocytes and Ly6C^{Int}Ly6G^{+}regulatory myeloid cells. Representative data from a WT mouse on d5 p.i. is shown in **B**. (**C**-**F**) Cells were harvested from VACV-infected WT or TCRδ$^{-/-}$ mice to analyze the recruitment of Ly6C^{+}Ly6G^{-} and Ly6C^{+}Ly6G^{+} monocyte populations. (**C**, **D**) Quantification of Ly6C^{+}Ly6G^{-} inflammatory monocytes on d5 (**C**) and d8 (**D**) post-infection in WT vs TCRδ$^{-/-}$ mice. (**E**, **F**) Quantification of Ly6C^{+}Ly6G^{+} monocytes on d5 (**E**) and d8 (**F**) post-infection in WT vs TCRδ$^{-/-}$ mice. All values depict the number of cells per pair of ears. Data in (**B**-**F**) are representative of 6 pairs of ears per group from 3 independent experiments. (**G-J**) WT (**G**, **I**) or TCRδ$^{-/-}$ (**H**, **J**) mice were infected i.d. with 10^4 PFU VACV-GFP per ear, ears harvested and frozen on d8 post-infection. Tissue sections were cut, stained with antibodies to GFP (in green) and either Ly6C (**G**,**H**) or Ly6G (**I**, **J**) (in blue) and visualized by deconvolution microscopy. Each image is representative of 4 ears per group from 2 experiments.

Figure 5. IFN-γ produced early after VACV infection, independent of γδ T cells, is required to control local tissue pathology but not local VACV replication or systemic virus spread. WT (**A, B, C, E, F**, **H**-**P**), TCRδ$^{-/-}$ (**N**) or IFN-γR$^{-/-}$ (**B, D, E, G, H-K**) mice were infected i.d. in the ear pinnae with 10^4 pfu of VACV and ears harvested and dissociated for analysis. (**A**) Time course of IFN-γ mRNA expression, measured by qPCR, in the ear after VACV infection. Data are representative of 3 independent experiments, showing the mean ± SEM of 3 or 4 biological replicates in each. Tissue swelling (**B**) was assessed through 6 days post infection. The

appearance of lesions in WT (**C**) or IFN-$\gamma R^{-/-}$ (**D**) mice was visualized 8 days after infection, and lesion size quantified (**E**) through 21 days post infection. The ensuing tissue loss in WT (**F**) or IFN-$\gamma R^{-/-}$ (**G**) mice was visualized 14 days after infection and quantified (**H**) through 21 days post infection. Data in (**B, E and H**) depict the mean ± SEM of 30 ears per group from 3 independent experiments. On d5 (**I-K**) post-infection, pairs of ears (**I**), spleen (**J**) and ovaries (**K**) were harvested from infected WT and IFN-$\gamma R^{-/-}$ mice to measure titers of VACV by plaque assay. Data is representative of 7 pairs of ovaries and ears, and 7 spleens, per group from 3 independent experiments. (**L**) Production of IFN-γ by $V\gamma3^+$ DETC, $V\gamma2^+$ or $V\gamma2^-V\gamma3^-$ dermal $\gamma\delta$ T cells from ear (gated as in **Fig. 1**) or by lymph node T_{CD4+} or T_{CD8+} (**M**) on d4 post-VACV infection in the presence of absence of PMA-ionomycin activation. Data in **L** and **M** are representative of 12 separate biological replicates from 3 independent experiments. (**N**) The relative IFN-γ mRNA expression in the ear of WT or TCR$\delta^{-/-}$ mice 4d after i.d. VACV infection. Data show the mean ± SEM of data from 3 independent experiments with 3 biological replicates in each. Representative data (**O**) and compiled and quantified total data from 3 independent experiments with 3 biological replicates in each (**P**) of intracellular cytokine staining of IFN-γ within $EpCAM^+CD45^-$ KC, $EpCAM^+CD45^+$ resident immune cells and $EpCAM^-CD45^+$ recruited immune populations. *p<0.05, **p<0.005, ***p<0.0001 by Student's t-test

Figure 6. Specific subsets of γδ T cells produce IL-17A upon cutaneous VACV infection. WT (**A**-**E**) or TCR$\delta^{-/-}$ (**E**) mice were infected i.d. in the ear pinnae with 10^4 pfu of VACV. (**A**) Expression of *il17a* mRNA in the ear of VACV-infected or uninfected WT mice. (**B**-**D**) Gating strategies are as shown in Figure 1. Production of IL-17A by $\gamma\delta$ T cells (**B**), or by $V\gamma3^+$ DETC, $V\gamma2^+$ or $V\gamma2^-V\gamma3^-$ dermal $\gamma\delta$ T cells (**C**) on d4 post-VACV infection in the presence of absence of PMA-ionomycin activation. (**D**) Quantitation of the numbers of cells displaying intracellular cytokine staining of IL-17A within $V\gamma3^+$ DETC, $V\gamma2^+$ or $V\gamma2^-V\gamma3^-$ dermal $\gamma\delta$ T cells populations on d4 post-

infection. (**E**) Expression of *il17a* mRNA in the ear of VACV-infected or uninfected WT or TCR$\delta^{-/-}$ mice, as shown, on d5 post-infection. Data are representative of 12 separate biological replicates from 3 independent experiments (**A**-**E**).

Figure 7. There is a wound healing signature induced in the ear of VACV infected mice. WT mice were infected i.d. in the ear pinnae with 10^4 pfu of VACV, ears harvested on d5 post-infection and mRNA levels of target molecules measured using Qiagen qPCR array plates as described in the methods sections. (**A**) Expression of cytokines and chemokines, and interferons and receptors, displayed using volcano plots, which demonstrate statistically significant points if above the p=0.05 line. Gene expression changes in WT mice in response to VACV, with genes that are upregulated >2-fold by VACV infection in the upper right hand quadrant and genes that are downregulated > 2-fold by VACV infection in the upper left hand quadrant. Genes that are significantly (> 2-fold, $p<0.05$) upregulated and have a defined role in wound healing are shown in red, and those that are significantly (> 2-fold, $p<0.05$) downregulated and have a defined role in wound healing are shown in blue. (**B**-**F**) Representative plots from the data displayed in (**A**), showing changes in mRNA levels on d5 post VACV-infection in genes associated with wound healing, including CC chemokines (**B**), IL-10 superfamily members (**C**), other cytokines and cytokine receptor antagonists (**D**), growth factors, hormones and their receptors (**E**) and TGF-β superfamily members (**F**). n=28 naïve, 29 VACV-infected mice per group.

Figure 8 Expression of wound healing molecules is altered in the absence of γδ T cells. WT or TCR$\delta^{-/-}$ (**A**-**C**, **J**, **P**, **R**), IL-22-TdTomato reporter (**D**-**I**) or IL-10GFP reporter (**K**-**P**) mice were infected i.d. in the ear pinnae with 10^4 pfu of VACV, ears harvested on d5 post-infection and (**A**-**C**) mRNA levels of target molecules, production of IL-22 (**D-I**) or IL-10 (**K**-**P**) by resident or recruited cell populations from the ear, or bulk mRNA expression levels of il22 (**J**), fgf9 (**Q**) or fgf7

(KGF, **R**) measured. (**A**-**C**) Expression of cytokines and chemokines, displayed using volcano plots, which demonstrate statistically significant points if above the p=0.05 line. (**A**) Cytokines and chemokines that are regulated in uninfected TCR$\delta^{-/-}$ mice relative to WT mice, showing genes that are upregulated >2-fold in uninfected TCR$\delta^{-/-}$ mice in the upper right hand quadrant and genes that are downregulated > 2-fold in uninfected TCR$\delta^{-/-}$ mice in the upper left hand quadrant. (**B**) Gene expression changes in VACV-infected TCR$\delta^{-/-}$ mice relative to uninfected TCR$\delta^{-/-}$ mice, with genes that are upregulated >2-fold by VACV infection of TCR$\delta^{-/-}$ mice in the upper right hand quadrant and genes that are downregulated > 2-fold by VACV infection of TCR$\delta^{-/-}$ mice in the upper left hand quadrant. (C) Gene expression changes in VACV-infected TCR$\delta^{-/-}$ mice relative to VACV infected WT, with genes that are upregulated >2-fold in TCR$\delta^{-/-}$ mice in the upper right hand quadrant and genes that are downregulated > 2-fold in TCR$\delta^{-/-}$ mice in the upper left hand quadrant. (**A**-**C**) Genes that are downregulated in VACV-infected TCR$\delta^{-/-}$ mice relative to VACV-infected WT mice (*il10* and *il22*) are displayed in green to facilitate ease of recognition in each plot. (**D**-**I**) Ears of IL-22-TdTomato reporter infected with VACV-GFP were harvested on d5 post-infection and dissociated to yield single cell suspensions, then stained to identify resident or recruited cell populations. Density plots show infection (marked by VACV-GFP) vs. IL-22 production (marked by TdTomato expression) within EpCAM^{+}CD45^{-} KC (**D**), resident immune cells (EpCAM^{+}CD45^{+}, **E**) and resident $\gamma\delta$ T cells (EpCAM^{+}CD45$^{+}\gamma\delta$TCR^{+}, **F**), recruited immune cell populations (EpCAM^{-}CD45^{+}, **G**), recruited lymphocytes (EpCAM^{-}CD45^{+}CD11b$^{-}\gamma\delta$ TCR^{-}, **H**) and recruited $\gamma\delta$ T cells (EpCAM^{-}CD45$^{+}\gamma\delta$TCR^{+}, **I**). (**J**) Expression of *il22* in ear tissue of uninfected or VACV-infected WT or TCR$\delta^{-/-}$ mice 5 dpi measured by RT-qPCR. (**K**-**P**) Ears of WT (**K**) or IL-10-GFP reporter (**L**-**P**) mice infected with VACV were harvested on d5 post-infection and dissociated to yield single cell suspensions, then stained to identify resident or recruited cell populations. Dot plots show IL-10 expression, (marked by GFP) in CD45+ from WT (**K**) or IL-10-GFP reporter mice (**L**). Density plots show CD45 vs. IL-10 production (marked by GFP) within

910 resident (EpCAM^{+}CD45^{+}, **M**, **N**) or recruited (EpCAM^{-}CD45^{+}, **O**, **P**) immune populations,
911 separated into γδ T cells (γδTCR^{+}, **M**, **O**) and myeloid cell populations (CD11b, γδTCR^{-}, **N**, **P**). (**Q,**
912 **R**) Expression of *fgf9* (**Q**) or *fgf7*(**R**) (which encodes KGF) in ear tissue of uninfected or VACV-
913 infected WT or TCRδ$^{-/-}$ mice 5 dpi measured by RT-qPCR.

914 **References**

915 1. Liu L, Zhong Q, Tian T, Dubin K, Athale SK, Kupper TS. Epidermal injury and
916 infection during poxvirus immunization is crucial for the generation of highly protective T
917 cell-mediated immunity. Nature medicine. 2010;16(2):224-7. Epub 2010/01/19. doi:
918 10.1038/nm.2078. PubMed PMID: 20081864; PubMed Central PMCID: PMC3070948.
919 2. Damaso CR, Esposito JJ, Condit RC, Moussatche N. An emergent poxvirus from
920 humans and cattle in Rio de Janeiro State: Cantagalo virus may derive from Brazilian
921 smallpox vaccine. Virology. 2000;277(2):439-49. Epub 2000/11/18. doi:
922 10.1006/viro.2000.0603. PubMed PMID: 11080491.
923 3. Tscharke DC, Smith GL. A model for vaccinia virus pathogenesis and immunity
924 based on intradermal injection of mouse ear pinnae. J Gen Virol. 1999;80 (Pt 10):2751-
925 5. PubMed PMID: 10573171.
926 4. Tscharke DC, Reading PC, Smith GL. Dermal infection with vaccinia virus reveals
927 roles for virus proteins not seen using other inoculation routes. J Gen Virol. 2002;83(Pt
928 8):1977-86. PubMed PMID: 12124461.
929 5. Reynolds MG, Holman RC, Yorita Christensen KL, Cheek JE, Damon IK. The
930 Incidence of Molluscum contagiosum among American Indians and Alaska Natives. PLoS
931 ONE. 2009;4(4):e5255. Epub 2009/04/22. doi: 10.1371/journal.pone.0005255. PubMed
932 PMID: 19381289; PubMed Central PMCID: PMC2667635.
933 6. Vos T, Flaxman AD, Naghavi M, Lozano R, Michaud C, Ezzati M, et al. Years lived
934 with disability (YLDs) for 1160 sequelae of 289 diseases and injuries 1990-2010: a
935 systematic analysis for the Global Burden of Disease Study 2010. Lancet.
936 2012;380(9859):2163-96. Epub 2012/12/19. doi: 10.1016/S0140-6736(12)61729-2.
937 PubMed PMID: 23245607.

938 7. Selin LK, Santolucito PA, Pinto AK, Szomolanyi-Tsuda E, Welsh RM. Innate
939 immunity to viruses: control of vaccinia virus infection by gamma delta T cells. J Immunol.
940 2001;166(11):6784-94. PubMed PMID: 11359837.
941 8. Agrati C, Castilletti C, De Santis R, Cimini E, Bordi L, Malkovsky M, et al.
942 Interferon-gamma-mediated antiviral immunity against orthopoxvirus infection is provided
943 by gamma delta T cells. J Infect Dis. 2006;193(11):1606-7; author reply 7-8. doi:
944 10.1086/503438. PubMed PMID: 16652291.
945 9. Welsh RM, Lin MY, Lohman BL, Varga SM, Zarozinski CC, Selin LK. Alpha beta
946 and gamma delta T-cell networks and their roles in natural resistance to viral infections.
947 Immunol Rev. 1997;159:79-93. PubMed PMID: 9416504.
948 10. Bukowski JF, Morita CT, Brenner MB. Recognition and destruction of virus-
949 infected cells by human gamma-delta CTL. Journal of Immunology. 1994;153:5133-40.
950 11. Fischer MA, Davies ML, Reider IE, Heipertz EL, Epler MR, Sei JJ, et al. CD11b(+),
951 Ly6G(+) cells produce type I interferon and exhibit tissue protective properties following
952 peripheral virus infection. PLoS Pathog. 2011;7(11):e1002374. doi:
953 10.1371/journal.ppat.1002374. PubMed PMID: 22102816; PubMed Central PMCID:
954 PMC3213107.
955 12. Davies ML, Parekh NJ, Kaminsky LW, Soni C, Reider IE, Krouse TE, et al. A
956 systemic macrophage response is required to contain a peripheral poxvirus infection.
957 PLoS Pathog. 2017;13(6):e1006435. doi: 10.1371/journal.ppat.1006435. PubMed PMID:
958 28614386; PubMed Central PMCID: PMCPMC5484545.
959 13. Parekh NJ, Krouse TE, Reider IE, Hobbs RP, Ward BM, Norbury CC. Type I
960 interferon-dependent CCL4 is induced by a cGAS/STING pathway that bypasses viral

961 inhibition and protects infected tissue, independent of viral burden. PLoS Pathog.
962 2019;15(10):e1007778. doi: 10.1371/journal.ppat.1007778. PubMed PMID: 31603920.
963 14. Garman RD, Ko JL, Vulpe CD, Raulet DH. T-cell receptor variable region gene
964 usage in T-cell populations. Proc Natl Acad Sci U S A. 1986;83(11):3987-91. Epub
965 1986/06/01. doi: 10.1073/pnas.83.11.3987. PubMed PMID: 3487085; PubMed Central
966 PMCID: PMCPMC323650.
967 15. O'Brien RL, Born WK. Dermal gammadelta T cells--What have we learned? Cell
968 Immunol. 2015;296(1):62-9. Epub 2015/02/05. doi: 10.1016/j.cellimm.2015.01.011.
969 PubMed PMID: 25649119; PubMed Central PMCID: PMCPMC4466165.
970 16. Cai Y, Xue F, Fleming C, Yang J, Ding C, Ma Y, et al. Differential developmental
971 requirement and peripheral regulation for dermal Vgamma4 and Vgamma6T17 cells in
972 health and inflammation. Nat Commun. 2014;5:3986. Epub 2014/06/10. doi:
973 10.1038/ncomms4986. PubMed PMID: 24909159; PubMed Central PMCID:
974 PMCPMC4068267.
975 17. Tuero I, Venzon D, Robert-Guroff M. Mucosal and Systemic gammadelta+ T Cells
976 Associated with Control of Simian Immunodeficiency Virus Infection. J Immunol.
977 2016;197(12):4686-95. Epub 2016/11/07. doi: 10.4049/jimmunol.1600579. PubMed
978 PMID: 27815422; PubMed Central PMCID: PMCPMC5136305.
979 18. Agrati C, Castilletti C, Cimini E, Romanelli A, Lapa D, Quartu S, et al. Antiviral
980 activity of human Vdelta2 T-cells against WNV includes both cytolytic and non-cytolytic
981 mechanisms. New Microbiol. 2016;39(2):139-42. Epub 2016/05/20. PubMed PMID:
982 27196553.

19. Liu W, Moussawi M, Roberts B, Boyson JE, Huber SA. Cross-regulation of T regulatory-cell response after coxsackievirus B3 infection by NKT and gammadelta T cells in the mouse. Am J Pathol. 2013;183(2):441-9. Epub 2013/06/12. doi: 10.1016/j.ajpath.2013.04.015. PubMed PMID: 23746656; PubMed Central PMCID: PMCPMC3730787.

20. Qin G, Liu Y, Zheng J, Xiang Z, Ng IH, Malik Peiris JS, et al. Phenotypic and functional characterization of human gammadelta T-cell subsets in response to influenza A viruses. J Infect Dis. 2012;205(11):1646-53. Epub 2012/03/30. doi: 10.1093/infdis/jis253. PubMed PMID: 22457284.

21. Ribot JC, Chaves-Ferreira M, d'Orey F, Wencker M, Goncalves-Sousa N, Decalf J, et al. Cutting edge: adaptive versus innate receptor signals selectively control the pool sizes of murine IFN-gamma- or IL-17-producing gammadelta T cells upon infection. Journal of immunology. 2010;185(11):6421-5. Epub 2010/11/03. doi: 10.4049/jimmunol.1002283. PubMed PMID: 21037088.

22. Lochner M, Peduto L, Cherrier M, Sawa S, Langa F, Varona R, et al. In vivo equilibrium of proinflammatory IL-17+ and regulatory IL-10+ Foxp3+ RORgamma t+ T cells. J Exp Med. 2008;205(6):1381-93. Epub 2008/05/28. doi: 10.1084/jem.20080034. PubMed PMID: 18504307; PubMed Central PMCID: PMCPMC2413035.

23. Lockhart E, Green AM, Flynn JL. IL-17 production is dominated by gammadelta T cells rather than CD4 T cells during Mycobacterium tuberculosis infection. J Immunol. 2006;177(7):4662-9. Epub 2006/09/20. doi: 10.4049/jimmunol.177.7.4662. PubMed PMID: 16982905.

1005 24. MacLeod AS, Hemmers S, Garijo O, Chabod M, Mowen K, Witherden DA, et al.
1006 Dendritic epidermal T cells regulate skin antimicrobial barrier function. The Journal of
1007 clinical investigation. 2013;123(10):4364-74. Epub 2013/09/21. doi: 10.1172/JCI70064.
1008 PubMed PMID: 24051381; PubMed Central PMCID: PMC3784546.
1009 25. Cho JS, Pietras EM, Garcia NC, Ramos RI, Farzam DM, Monroe HR, et al. IL-17
1010 is essential for host defense against cutaneous Staphylococcus aureus infection in mice.
1011 J Clin Invest. 2010;120(5):1762-73. Epub 2010/04/07. doi: 10.1172/JCI40891. PubMed
1012 PMID: 20364087; PubMed Central PMCID: PMCPMC2860944.
1013 26. Rani M, Zhang Q, Scherer MR, Cap AP, Schwacha MG. Activated skin
1014 gammadelta T-cells regulate T-cell infiltration of the wound site after burn. Innate Immun.
1015 2015;21(2):140-50. Epub 2014/01/15. doi: 10.1177/1753425913519350. PubMed PMID:
1016 24412847.
1017 27. Petrovic J, Silva JR, Bannerman CA, Segal JP, Marshall AS, Haird CM, et al.
1018 gammadelta T Cells Modulate Myeloid Cell Recruitment but Not Pain During Peripheral
1019 Inflammation. Front Immunol. 2019;10:473. Epub 2019/04/03. doi:
1020 10.3389/fimmu.2019.00473. PubMed PMID: 30936874; PubMed Central PMCID:
1021 PMCPMC6431614.
1022 28. Li H, Xiang Z, Feng T, Li J, Liu Y, Fan Y, et al. Human Vgamma9Vdelta2-T cells
1023 efficiently kill influenza virus-infected lung alveolar epithelial cells. Cell Mol Immunol.
1024 2013;10(2):159-64. Epub 2013/01/29. doi: 10.1038/cmi.2012.70. PubMed PMID:
1025 23353835; PubMed Central PMCID: PMCPMC4003054.
1026 29. Zhao Y, Lin L, Xiao Z, Li M, Wu X, Li W, et al. Protective Role of gammadelta T
1027 Cells in Different Pathogen Infections and Its Potential Clinical Application. J Immunol

1028 Res. 2018;2018:5081634. Epub 2018/08/18. doi: 10.1155/2018/5081634. PubMed PMID:
1029 30116753; PubMed Central PMCID: PMCPMC6079409.
1030 30. Komori HK, Witherden DA, Kelly R, Sendaydiego K, Jameson JM, Teyton L, et al.
1031 Cutting edge: dendritic epidermal gammadelta T cell ligands are rapidly and locally
1032 expressed by keratinocytes following cutaneous wounding. J Immunol.
1033 2012;188(7):2972-6. Epub 2012/03/07. doi: 10.4049/jimmunol.1100887. PubMed PMID:
1034 22393149; PubMed Central PMCID: PMCPMC3311739.
1035 31. Girardi M, Lewis JM, Filler RB, Hayday AC, Tigelaar RE. Environmentally
1036 responsive and reversible regulation of epidermal barrier function by gammadelta T cells.
1037 J Invest Dermatol. 2006;126(4):808-14. Epub 2006/01/28. doi: 10.1038/sj.jid.5700120.
1038 PubMed PMID: 16439970.
1039 32. Jameson JM, Cauvi G, Witherden DA, Havran WL. A keratinocyte-responsive
1040 gamma delta TCR is necessary for dendritic epidermal T cell activation by damaged
1041 keratinocytes and maintenance in the epidermis. J Immunol. 2004;172(6):3573-9. Epub
1042 2004/03/09. doi: 10.4049/jimmunol.172.6.3573. PubMed PMID: 15004158.
1043 33. Whang MI, Guerra N, Raulet DH. Costimulation of dendritic epidermal gammadelta
1044 T cells by a new NKG2D ligand expressed specifically in the skin. J Immunol.
1045 2009;182(8):4557-64. Epub 2009/04/04. doi: 10.4049/jimmunol.0802439. PubMed PMID:
1046 19342629; PubMed Central PMCID: PMCPMC3001286.
1047 34. Anderson LS, Yu S, Rivara KR, Reynolds MB, Hernandez AA, Wu X, et al.
1048 CCR6(+) gammadelta T Cells Home to Skin Wounds and Restore Normal Wound Healing
1049 in CCR6-Deficient Mice. J Invest Dermatol. 2019;139(9):2061-4 e2. Epub 2019/04/03.

1050 doi: 10.1016/j.jid.2019.02.032. PubMed PMID: 30935975; PubMed Central PMCID:
1051 PMCPMC6708754.
1052 35. Bonneville M. Semaphorins: new cues for skin healing by gammadelta T cells.
1053 Immunity. 2012;37(2):194-6. Epub 2012/08/28. doi: 10.1016/j.immuni.2012.08.003.
1054 PubMed PMID: 22921116.
1055 36. Toulon A, Breton L, Taylor KR, Tenenhaus M, Bhavsar D, Lanigan C, et al. A role
1056 for human skin-resident T cells in wound healing. J Exp Med. 2009;206(4):743-50. Epub
1057 2009/03/25. doi: 10.1084/jem.20081787. PubMed PMID: 19307328; PubMed Central
1058 PMCID: PMCPMC2715110.
1059 37. Li Y, Wu J, Luo G, He W. Functions of Vgamma4 T Cells and Dendritic Epidermal
1060 T Cells on Skin Wound Healing. Front Immunol. 2018;9:1099. Epub 2018/06/20. doi:
1061 10.3389/fimmu.2018.01099. PubMed PMID: 29915573; PubMed Central PMCID:
1062 PMCPMC5994537.
1063 38. Krishnan S, Prise IE, Wemyss K, Schenck LP, Bridgeman HM, McClure FA, et al.
1064 Amphiregulin-producing gammadelta T cells are vital for safeguarding oral barrier
1065 immune homeostasis. Proc Natl Acad Sci U S A. 2018;115(42):10738-43. Epub
1066 2018/10/04. doi: 10.1073/pnas.1802320115. PubMed PMID: 30279177; PubMed Central
1067 PMCID: PMCPMC6196490.
1068 39. Gay D, Kwon O, Zhang Z, Spata M, Plikus MV, Holler PD, et al. Fgf9 from dermal
1069 gammadelta T cells induces hair follicle neogenesis after wounding. Nat Med.
1070 2013;19(7):916-23. Epub 2013/06/04. doi: 10.1038/nm.3181. PubMed PMID: 23727932;
1071 PubMed Central PMCID: PMCPMC4054871.

1072 40. Xu P, Fu X, Xiao N, Guo Y, Pei Q, Peng Y, et al. Involvements of gammadeltaT
1073 Lymphocytes in Acute and Chronic Skin Wound Repair. Inflammation. 2017;40(4):1416-
1074 27. Epub 2017/05/26. doi: 10.1007/s10753-017-0585-6. PubMed PMID: 28540539.
1075 41. Havran WL, Jameson JM. Epidermal T cells and wound healing. J Immunol.
1076 2010;184(10):5423-8. Epub 2010/05/21. doi: 10.4049/jimmunol.0902733. PubMed PMID:
1077 20483798; PubMed Central PMCID: PMCPMC2944652.
1078 42. Jameson J, Havran WL. Skin gammadelta T-cell functions in homeostasis and
1079 wound healing. Immunol Rev. 2007;215:114-22. Epub 2007/02/13. doi: 10.1111/j.1600-
1080 065X.2006.00483.x. PubMed PMID: 17291283.
1081 43. Macleod AS, Havran WL. Functions of skin-resident gammadelta T cells. Cell Mol
1082 Life Sci. 2011;68(14):2399-408. Epub 2011/05/12. doi: 10.1007/s00018-011-0702-x.
1083 PubMed PMID: 21560071; PubMed Central PMCID: PMCPMC3123394.
1084 44. Jameson J, Ugarte K, Chen N, Yachi P, Fuchs E, Boismenu R, et al. A role for skin
1085 gammadelta T cells in wound repair. Science. 2002;296(5568):747-9. Epub 2002/04/27.
1086 doi: 10.1126/science.1069639. PubMed PMID: 11976459.
1087 45. Khairallah C, Chu TH, Sheridan BS. Tissue Adaptations of Memory and Tissue-
1088 Resident Gamma Delta T Cells. Front Immunol. 2018;9:2636. Epub 2018/12/13. doi:
1089 10.3389/fimmu.2018.02636. PubMed PMID: 30538697; PubMed Central PMCID:
1090 PMCPMC6277633.
1091 46. Serhan CN, Yacoubian S, Yang R. Anti-inflammatory and proresolving lipid
1092 mediators. Annual review of pathology. 2008;3:279-312. doi:
1093 10.1146/annurev.pathmechdis.3.121806.151409. PubMed PMID: 18233953; PubMed
1094 Central PMCID: PMC2739396.

1095 47. Serhan CN, Chiang N, Van Dyke TE. Resolving inflammation: dual anti-
1096 inflammatory and pro-resolution lipid mediators. Nat Rev Immunol. 2008;8(5):349-61. doi:
1097 10.1038/nri2294. PubMed PMID: 18437155; PubMed Central PMCID: PMC2744593.
1098 48. Tikoo S, Jain R, Kurz AR, Weninger W. The lymphoid cell network in the skin.
1099 Immunol Cell Biol. 2018;96(5):485-96. Epub 2018/02/20. doi: 10.1111/imcb.12026.
1100 PubMed PMID: 29457268.
1101 49. Lloyd JB, Gill HS, Haig DM, Husband AJ. In vivo T-cell subset depletion suggests
1102 that CD4+ T-cells and a humoral immune response are important for the elimination of
1103 orf virus from the skin of sheep. Vet Immunol Immunopathol. 2000;74(3-4):249-62. Epub
1104 2000/05/10. doi: 10.1016/s0165-2427(00)00178-1. PubMed PMID: 10802292.
1105 50. Worku S, Gorse GJ, Belshe RB, Hoft DF. Canarypox vaccines induce antigen-
1106 specific human gammadelta T cells capable of interferon-gamma production. J Infect Dis.
1107 2001;184(5):525-32. Epub 2001/07/28. doi: 10.1086/322792. PubMed PMID: 11474428.
1108 51. Anderson IE, Reid HW, Nettleton PF, McInnes CJ, Haig DM. Detection of cellular
1109 cytokine mRNA expression during orf virus infection in sheep: differential interferon-
1110 gamma mRNA expression by cells in primary versus reinfection skin lesions. Vet Immunol
1111 Immunopathol. 2001;83(3-4):161-76. Epub 2001/12/04. doi: 10.1016/s0165-
1112 2427(01)00388-9. PubMed PMID: 11730927.
1113 52. Gulbahar MY, Davis WC, Yuksel H, Cabalar M. Immunohistochemical evaluation
1114 of inflammatory infiltrate in the skin and lung of lambs naturally infected with sheeppox
1115 virus. Vet Pathol. 2006;43(1):67-75. Epub 2006/01/13. doi: 10.1354/vp.43-1-67. PubMed
1116 PMID: 16407491.

1117 53. Gierynska M, Pawlak E, Schollenberger A, Cespedes IS. Dendritic epidermal T
1118 cells: their role in the early phase of ectromelia virus infection. Postepy Hig Med Dosw
1119 (Online). 2009;63:369-76. Epub 2009/09/03. PubMed PMID: 19724077.
1120 54. Jacobs N, Chen RA, Gubser C, Najarro P, Smith GL. Intradermal immune
1121 response after infection with Vaccinia virus. J Gen Virol. 2006;87(5):1157-61. PubMed
1122 PMID: 16603516.
1123 55. Hickman HD, Reynoso GV, Ngudiankama BF, Cush SS, Gibbs J, Bennink JR, et
1124 al. CXCR3 chemokine receptor enables local CD8(+) T cell migration for the destruction
1125 of virus-infected cells. Immunity. 2015;42(3):524-37. doi: 10.1016/j.immuni.2015.02.009.
1126 PubMed PMID: 25769612; PubMed Central PMCID: PMCPMC4365427.
1127 56. Hickman HD, Li L, Reynoso GV, Rubin EJ, Skon CN, Mays JW, et al. Chemokines
1128 control naive CD8+ T cell selection of optimal lymph node antigen presenting cells. The
1129 Journal of experimental medicine. 2011;208(12):2511-24. Epub 2011/11/02. doi:
1130 10.1084/jem.20102545. PubMed PMID: 22042976; PubMed Central PMCID:
1131 PMC3256957.
1132 57. Vantourout P, Hayday A. Six-of-the-best: unique contributions of gammadelta T
1133 cells to immunology. Nat Rev Immunol. 2013;13(2):88-100. Epub 2013/01/26. doi:
1134 10.1038/nri3384. PubMed PMID: 23348415; PubMed Central PMCID:
1135 PMCPMC3951794.
1136 58. Mullbacher A, Waring P, Tha Hla R, Tran T, Chin S, Stehle T, et al. Granzymes
1137 are the essential downstream effector molecules for the control of primary virus infections
1138 by cytolytic leukocytes. Proc Natl Acad Sci U S A. 1999;96(24):13950-5. PubMed PMID:
1139 10570179.

1140 59. Hickman HD, Reynoso GV, Ngudiankama BF, Rubin EJ, Magadan JG, Cush SS,
1141 et al. Anatomically restricted synergistic antiviral activities of innate and adaptive immune
1142 cells in the skin. Cell host & microbe. 2013;13(2):155-68. Epub 2013/02/19. doi:
1143 10.1016/j.chom.2013.01.004. PubMed PMID: 23414756; PubMed Central PMCID:
1144 PMC3591514.
1145 60. Betts MR, Nason MC, West SM, De Rosa SC, Migueles SA, Abraham J, et al. HIV
1146 nonprogressors preferentially maintain highly functional HIV-specific CD8+ T cells. Blood.
1147 2006;107(12):4781-9. Epub 2006/02/10. doi: 10.1182/blood-2005-12-4818. PubMed
1148 PMID: 16467198; PubMed Central PMCID: PMCPMC1895811.
1149 61. Davies ML, Sei JJ, Siciliano NA, Xu RH, Roscoe F, Sigal LJ, et al. MyD88-
1150 dependent immunity to a natural model of vaccinia virus infection does not involve Toll-
1151 like receptor 2. J Virol. 2014;88(6):3557-67. doi: 10.1128/JVI.02776-13. PubMed PMID:
1152 24403581; PubMed Central PMCID: PMC3957935.
1153 62. Scheynius A, Fransson J, Johansson C, Hammar H, Baker B, Fry L, et al.
1154 Expression of interferon-gamma receptors in normal and psoriatic skin. J Invest Dermatol.
1155 1992;98(2):255-8. Epub 1992/02/01. doi: 10.1111/1523-1747.ep12556086. PubMed
1156 PMID: 1531061.
1157 63. Shin JM, Choi DK, Sohn KC, Koh JW, Lee YH, Seo YJ, et al. Induction of alopecia
1158 areata in C3H/HeJ mice using polyinosinic-polycytidylic acid (poly[I:C]) and interferon-
1159 gamma. Sci Rep. 2018;8(1):12518. Epub 2018/08/23. doi: 10.1038/s41598-018-30997-
1160 3. PubMed PMID: 30131581; PubMed Central PMCID: PMCPMC6104095.
1161 64. Karupiah G, Blanden RV, Ramshaw IA. Interferon gamma is involved in the
1162 recovery of athymic nude mice from recombinant vaccinia virus/interleukin 2 infection. J

1163 Exp Med. 1990;172(5):1495-503. PubMed PMID: 2121889; PubMed Central PMCID:
1164 PMCPMC2188664.
1165 65. Jensen KD, Su X, Shin S, Li L, Youssef S, Yamasaki S, et al. Thymic selection
1166 determines gammadelta T cell effector fate: antigen-naive cells make interleukin-17 and
1167 antigen-experienced cells make interferon gamma. Immunity. 2008;29(1):90-100. Epub
1168 2008/07/01. doi: 10.1016/j.immuni.2008.04.022. PubMed PMID: 18585064; PubMed
1169 Central PMCID: PMCPMC2601709.
1170 66. Sumaria N, Roediger B, Ng LG, Qin J, Pinto R, Cavanagh LL, et al. Cutaneous
1171 immunosurveillance by self-renewing dermal gammadelta T cells. J Exp Med.
1172 2011;208(3):505-18. Epub 2011/02/23. doi: 10.1084/jem.20101824. PubMed PMID:
1173 21339323; PubMed Central PMCID: PMCPMC3058585.
1174 67. Pantelyushin S, Haak S, Ingold B, Kulig P, Heppner FL, Navarini AA, et al.
1175 Rorgammat+ innate lymphocytes and gammadelta T cells initiate psoriasiform plaque
1176 formation in mice. J Clin Invest. 2012;122(6):2252-6. Epub 2012/05/02. doi:
1177 10.1172/JCI61862. PubMed PMID: 22546855; PubMed Central PMCID:
1178 PMCPMC3366412.
1179 68. Cai Y, Shen X, Ding C, Qi C, Li K, Li X, et al. Pivotal role of dermal IL-17-producing
1180 gammadelta T cells in skin inflammation. Immunity. 2011;35(4):596-610. Epub
1181 2011/10/11. doi: 10.1016/j.immuni.2011.08.001. PubMed PMID: 21982596; PubMed
1182 Central PMCID: PMCPMC3205267.
1183 69. Gray EE, Ramirez-Valle F, Xu Y, Wu S, Wu Z, Karjalainen KE, et al. Deficiency in
1184 IL-17-committed Vgamma4(+) gammadelta T cells in a spontaneous Sox13-mutant
1185 CD45.1(+) congenic mouse substrain provides protection from dermatitis. Nat Immunol.

2013;14(6):584-92. Epub 2013/04/30. doi: 10.1038/ni.2585. PubMed PMID: 23624556; PubMed Central PMCID: PMCPMC3660499.

70. Gillitzer R, Goebeler M. Chemokines in cutaneous wound healing. J Leukoc Biol. 2001;69(4):513-21. Epub 2001/04/20. PubMed PMID: 11310836.

71. Werner S, Grose R. Regulation of wound healing by growth factors and cytokines. Physiol Rev. 2003;83(3):835-70. Epub 2003/07/05. doi: 10.1152/physrev.2003.83.3.835. PubMed PMID: 12843410.

72. Eming SA, Krieg T, Davidson JM. Inflammation in wound repair: molecular and cellular mechanisms. J Invest Dermatol. 2007;127(3):514-25. Epub 2007/02/15. doi: 10.1038/sj.jid.5700701. PubMed PMID: 17299434.

73. Penn JW, Grobbelaar AO, Rolfe KJ. The role of the TGF-beta family in wound healing, burns and scarring: a review. Int J Burns Trauma. 2012;2(1):18-28. Epub 2012/08/29. PubMed PMID: 22928164; PubMed Central PMCID: PMCPMC3415964.

74. Liarte S, Bernabe-Garcia A, Nicolas FJ. Role of TGF-beta in Skin Chronic Wounds: A Keratinocyte Perspective. Cells. 2020;9(2). Epub 2020/02/06. doi: 10.3390/cells9020306. PubMed PMID: 32012802; PubMed Central PMCID: PMCPMC7072438.

75. Savage AK, Liang HE, Locksley RM. The Development of Steady-State Activation Hubs between Adult LTi ILC3s and Primed Macrophages in Small Intestine. J Immunol. 2017;199(5):1912-22. Epub 2017/07/28. doi: 10.4049/jimmunol.1700155. PubMed PMID: 28747343; PubMed Central PMCID: PMCPMC5568484.

76. Madan R, Demircik F, Surianarayanan S, Allen JL, Divanovic S, Trompette A, et al. Nonredundant roles for B cell-derived IL-10 in immune counter-regulation. J Immunol.

2009;183(4):2312-20. Epub 2009/07/22. doi: 10.4049/jimmunol.0900185. PubMed PMID: 19620304; PubMed Central PMCID: PMCPMC2772089.

77. Cush SS, Reynoso GV, Kamenyeva O, Bennink JR, Yewdell JW, Hickman HD. Locally Produced IL-10 Limits Cutaneous Vaccinia Virus Spread. PLoS Pathog. 2016;12(3):e1005493. doi: 10.1371/journal.ppat.1005493. PubMed PMID: 26991092; PubMed Central PMCID: PMCPMC4798720.

78. Mirza R, DiPietro LA, Koh TJ. Selective and specific macrophage ablation is detrimental to wound healing in mice. Am J Pathol. 2009;175(6):2454-62. doi: 10.2353/ajpath.2009.090248. PubMed PMID: 19850888; PubMed Central PMCID: PMCPMC2789630.

79. Lin Q, Fang D, Fang J, Ren X, Yang X, Wen F, et al. Impaired wound healing with defective expression of chemokines and recruitment of myeloid cells in TLR3-deficient mice. J Immunol. 2011;186(6):3710-7. Epub 2011/02/15. doi: 10.4049/jimmunol.1003007. PubMed PMID: 21317384.

80. Gregorio J, Meller S, Conrad C, Di Nardo A, Homey B, Lauerma A, et al. Plasmacytoid dendritic cells sense skin injury and promote wound healing through type I interferons. The Journal of experimental medicine. 2010;207(13):2921-30. Epub 2010/12/01. doi: 10.1084/jem.20101102. PubMed PMID: 21115688; PubMed Central PMCID: PMC3005239.

81. Bhartiya D, Sklarsh JW, Maheshwari RK. Enhanced wound healing in animal models by interferon and an interferon inducer. J Cell Physiol. 1992;150(2):312-9. doi: 10.1002/jcp.1041500214. PubMed PMID: 1734035.

82. Daley JM, Thomay AA, Connolly MD, Reichner JS, Albina JE. Use of Ly6G-specific monoclonal antibody to deplete neutrophils in mice. J Leukoc Biol. 2008;83(1):64-70. PubMed PMID: 17884993.

83. Goren I, Christen U, Pfeilschifter J, Frank S. A heterogeneous Ly-6B2(+) leukocyte population consists of yet undescribed iNOS-expressing cell types in murine skin wounds. Nitric Oxide. 2018;74:23-31. Epub 2018/01/23. doi: 10.1016/j.niox.2018.01.004. PubMed PMID: 29355774.

84. Dunnill C, Patton T, Brennan J, Barrett J, Dryden M, Cooke J, et al. Reactive oxygen species (ROS) and wound healing: the functional role of ROS and emerging ROS-modulating technologies for augmentation of the healing process. Int Wound J. 2017;14(1):89-96. Epub 2015/12/22. doi: 10.1111/iwj.12557. PubMed PMID: 26688157.

85. Sutoh Y, Mohamed RH, Kasahara M. Origin and Evolution of Dendritic Epidermal T Cells. Front Immunol. 2018;9:1059. Epub 2018/06/06. doi: 10.3389/fimmu.2018.01059. PubMed PMID: 29868019; PubMed Central PMCID: PMCPMC5960712.

86. Woodward Davis AS, Bergsbaken T, Delaney MA, Bevan MJ. Dermal-resident versus recruited gammadelta T cell response to cutaneous vaccinia virus infection. J Immunol. 2015;194(5):2260-7. doi: 10.4049/jimmunol.1402438. PubMed PMID: 25609844; PubMed Central PMCID: PMCPMC4340759.

87. Ono T, Okamoto K, Nakashima T, Nitta T, Hori S, Iwakura Y, et al. IL-17-producing gammadelta T cells enhance bone regeneration. Nat Commun. 2016;7:10928. Epub 2016/03/12. doi: 10.1038/ncomms10928. PubMed PMID: 26965320; PubMed Central PMCID: PMCPMC4792964.

88. Griffin GK, Newton G, Tarrio ML, Bu DX, Maganto-Garcia E, Azcutia V, et al. IL-17 and TNF-alpha sustain neutrophil recruitment during inflammation through synergistic effects on endothelial activation. J Immunol. 2012;188(12):6287-99. Epub 2012/05/09. doi: 10.4049/jimmunol.1200385. PubMed PMID: 22566565; PubMed Central PMCID: PMCPMC3370121.

89. Grice EA, Segre JA. The skin microbiome. Nat Rev Microbiol. 2011;9(4):244-53. Epub 2011/03/17. doi: 10.1038/nrmicro2537. PubMed PMID: 21407241; PubMed Central PMCID: PMCPMC3535073.

90. Purzycka-Bohdan D, Szczerkowska-Dobosz A, Zablotna M, Wierzbicka J, Piotrowska A, Zmijewski MA, et al. Assessment of Interleukin 16 Serum Levels and Skin Expression in Psoriasis Patients in Correlation with Clinical Severity of the Disease. PLoS One. 2016;11(10):e0165577. Epub 2016/10/28. doi: 10.1371/journal.pone.0165577. PubMed PMID: 27788245; PubMed Central PMCID: PMCPMC5082815.

91. Shibata S, Tada Y, Asano Y, Hau CS, Kato T, Saeki H, et al. Adiponectin regulates cutaneous wound healing by promoting keratinocyte proliferation and migration via the ERK signaling pathway. J Immunol. 2012;189(6):3231-41. Epub 2012/08/21. doi: 10.4049/jimmunol.1101739. PubMed PMID: 22904306.

92. Rhodes KA, Andrew EM, Newton DJ, Tramonti D, Carding SR. A subset of IL-10-producing gammadelta T cells protect the liver from Listeria-elicited, CD8(+) T cell-mediated injury. Eur J Immunol. 2008;38(8):2274-83. Epub 2008/07/16. doi: 10.1002/eji.200838354. PubMed PMID: 18624301.

1274 93. Boniface K, Bernard FX, Garcia M, Gurney AL, Lecron JC, Morel F. IL-22 inhibits
1275 epidermal differentiation and induces proinflammatory gene expression and migration of
1276 human keratinocytes. J Immunol. 2005;174(6):3695-702. PubMed PMID: 15749908.
1277 94. Wise LM, Stuart GS, Real NC, Fleming SB, Mercer AA. Orf virus IL-10 accelerates
1278 wound healing while limiting inflammation and scarring. Wound Repair Regen.
1279 2014;22(3):356-67. Epub 2014/05/23. doi: 10.1111/wrr.12169. PubMed PMID:
1280 24844335.
1281 95. Bodaan CJ, Wise LM, Wakelin KA, Stuart GS, Real NC, Mercer AA, et al. Short-
1282 term treatment of equine wounds with orf virus IL-10 and VEGF-E dampens inflammation
1283 and promotes repair processes without accelerating closure. Wound Repair Regen.
1284 2016;24(6):966-80. Epub 2016/10/19. doi: 10.1111/wrr.12488. PubMed PMID:
1285 27681311.
1286 96. Bennett JR, Lateef Z, Fleming SB, Mercer AA, Wise LM. Orf virus IL-10 reduces
1287 monocyte, dendritic cell and mast cell recruitment to inflamed skin. Virus Res.
1288 2016;213:230-7. Epub 2016/01/07. doi: 10.1016/j.virusres.2015.12.015. PubMed PMID:
1289 26732486.
1290 97. Wise LM, Stuart GS, Jones NC, Fleming SB, Mercer AA. Orf Virus IL-10 and
1291 VEGF-E Act Synergistically to Enhance Healing of Cutaneous Wounds in Mice. J Clin
1292 Med. 2020;9(4). Epub 2020/04/16. doi: 10.3390/jcm9041085. PubMed PMID: 32290480;
1293 PubMed Central PMCID: PMCPMC7231296.
1294 98. Boniface K, Guignouard E, Pedretti N, Garcia M, Delwail A, Bernard FX, et al. A
1295 role for T cell-derived interleukin 22 in psoriatic skin inflammation. Clin Exp Immunol.

2007;150(3):407-15. Epub 2007/09/29. doi: 10.1111/j.1365-2249.2007.03511.x. PubMed PMID: 17900301; PubMed Central PMCID: PMCPMC2219373.

99. Ma HL, Liang S, Li J, Napierata L, Brown T, Benoit S, et al. IL-22 is required for Th17 cell-mediated pathology in a mouse model of psoriasis-like skin inflammation. J Clin Invest. 2008;118(2):597-607. Epub 2008/01/19. doi: 10.1172/JCI33263. PubMed PMID: 18202747; PubMed Central PMCID: PMCPMC2200300.

100. Ahlfors H, Morrison PJ, Duarte JH, Li Y, Biro J, Tolaini M, et al. IL-22 fate reporter reveals origin and control of IL-22 production in homeostasis and infection. J Immunol. 2014;193(9):4602-13. doi: 10.4049/jimmunol.1401244. PubMed PMID: 25261485; PubMed Central PMCID: PMCPMC4201943.

101. McGee HM, Schmidt BA, Booth CJ, Yancopoulos GD, Valenzuela DM, Murphy AJ, et al. IL-22 promotes fibroblast-mediated wound repair in the skin. J Invest Dermatol. 2013;133(5):1321-9. doi: 10.1038/jid.2012.463. PubMed PMID: 23223145; PubMed Central PMCID: PMCPMC3610794.

102. Avitabile S, Odorisio T, Madonna S, Eyerich S, Guerra L, Eyerich K, et al. Interleukin-22 Promotes Wound Repair in Diabetes by Improving Keratinocyte Pro-Healing Functions. J Invest Dermatol. 2015;135(11):2862-70. Epub 2015/07/15. doi: 10.1038/jid.2015.278. PubMed PMID: 26168231.

103. Kolumam G, Wu X, Lee WP, Hackney JA, Zavala-Solorio J, Gandham V, et al. IL-22R Ligands IL-20, IL-22, and IL-24 Promote Wound Healing in Diabetic db/db Mice. PLoS One. 2017;12(1):e0170639. doi: 10.1371/journal.pone.0170639. PubMed PMID: 28125663; PubMed Central PMCID: PMCPMC5268431 following competing interests: All authors are current or previous employees of Genentech. Genentech has reviewed the

manuscript, and may potentially file patents and develop therapies based on part of the data in the manuscript. However, this does not alter our adherence to PLOS ONE policies on sharing data and materials.

104. Lerman G, Sharon M, Leibowitz-Amit R, Sidi Y, Avni D. The crosstalk between IL-22 signaling and miR-197 in human keratinocytes. PLoS One. 2014;9(9):e107467. Epub 2014/09/11. doi: 10.1371/journal.pone.0107467. PubMed PMID: 25208211; PubMed Central PMCID: PMCPMC4160297.

105. Gimblet C, Loesche MA, Carvalho L, Carvalho EM, Grice EA, Artis D, et al. IL-22 Protects against Tissue Damage during Cutaneous Leishmaniasis. PLoS One. 2015;10(8):e0134698. Epub 2015/08/19. doi: 10.1371/journal.pone.0134698. PubMed PMID: 26285207; PubMed Central PMCID: PMCPMC4540492.

106. Itohara S, Mombaerts P, Lafaille J, Iacomini J, Nelson A, Clarke AR, et al. T cell receptor delta gene mutant mice: independent generation of alpha beta T cells and programmed rearrangements of gamma delta TCR genes. Cell. 1993;72(3):337-48. PubMed PMID: 8381716.

107. Norbury CC, Malide D, Gibbs JS, Bennink JR, Yewdell JW. Visualizing priming of virus-specific CD8+ T cells by infected dendritic cells in vivo. Nat Immunol. 2002;3(3):265-71. PubMed PMID: 11828323.

108. Hersperger AR, Siciliano NA, DeHaven BC, Snook AE, Eisenlohr LC. Epithelial immunization induces polyfunctional CD8+ T cells and optimal mousepox protection. J Virol. 2014;88(16):9472-5. doi: 10.1128/JVI.01464-14. PubMed PMID: 24899206; PubMed Central PMCID: PMCPMC4136261.

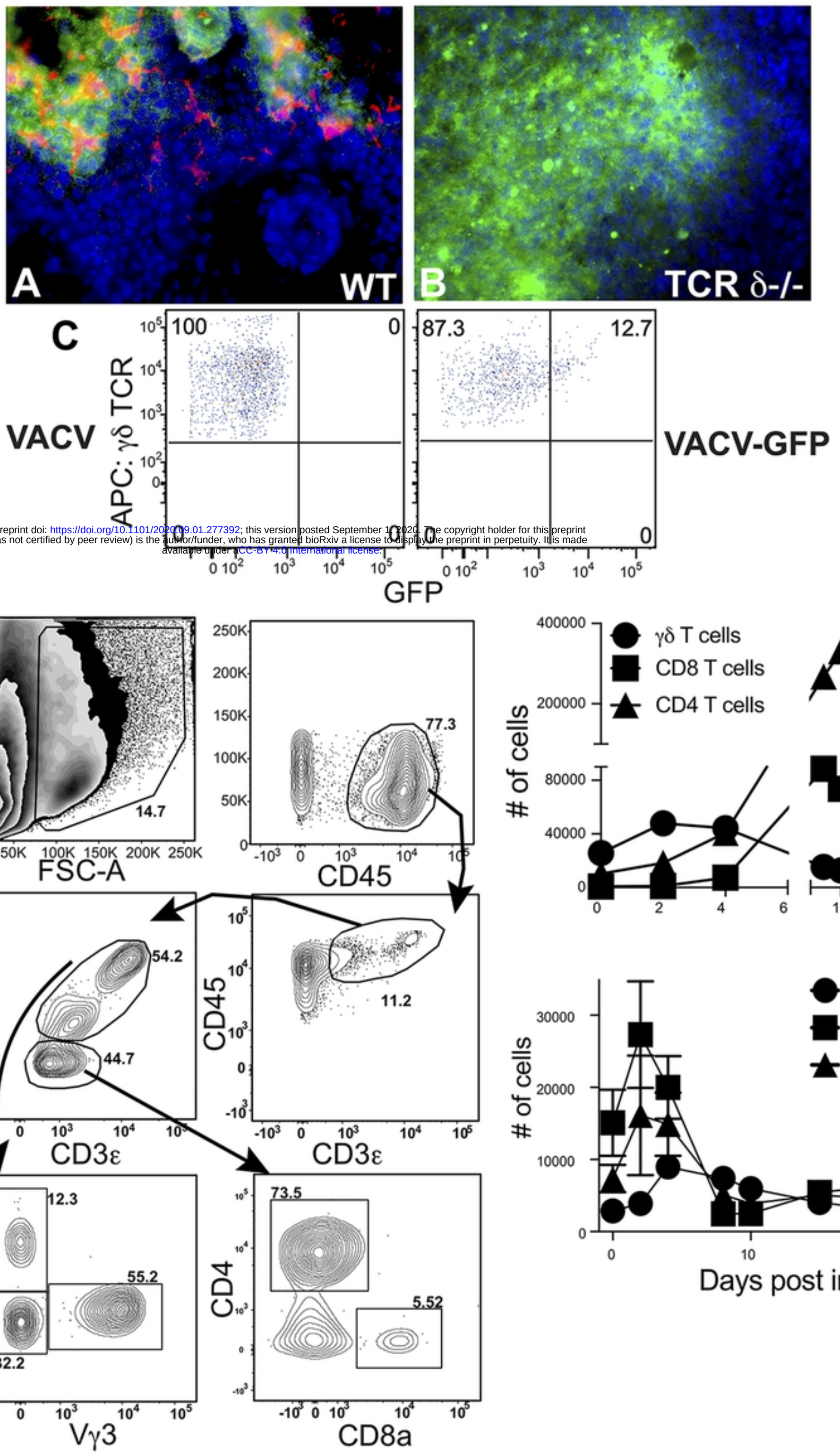

Figure 1

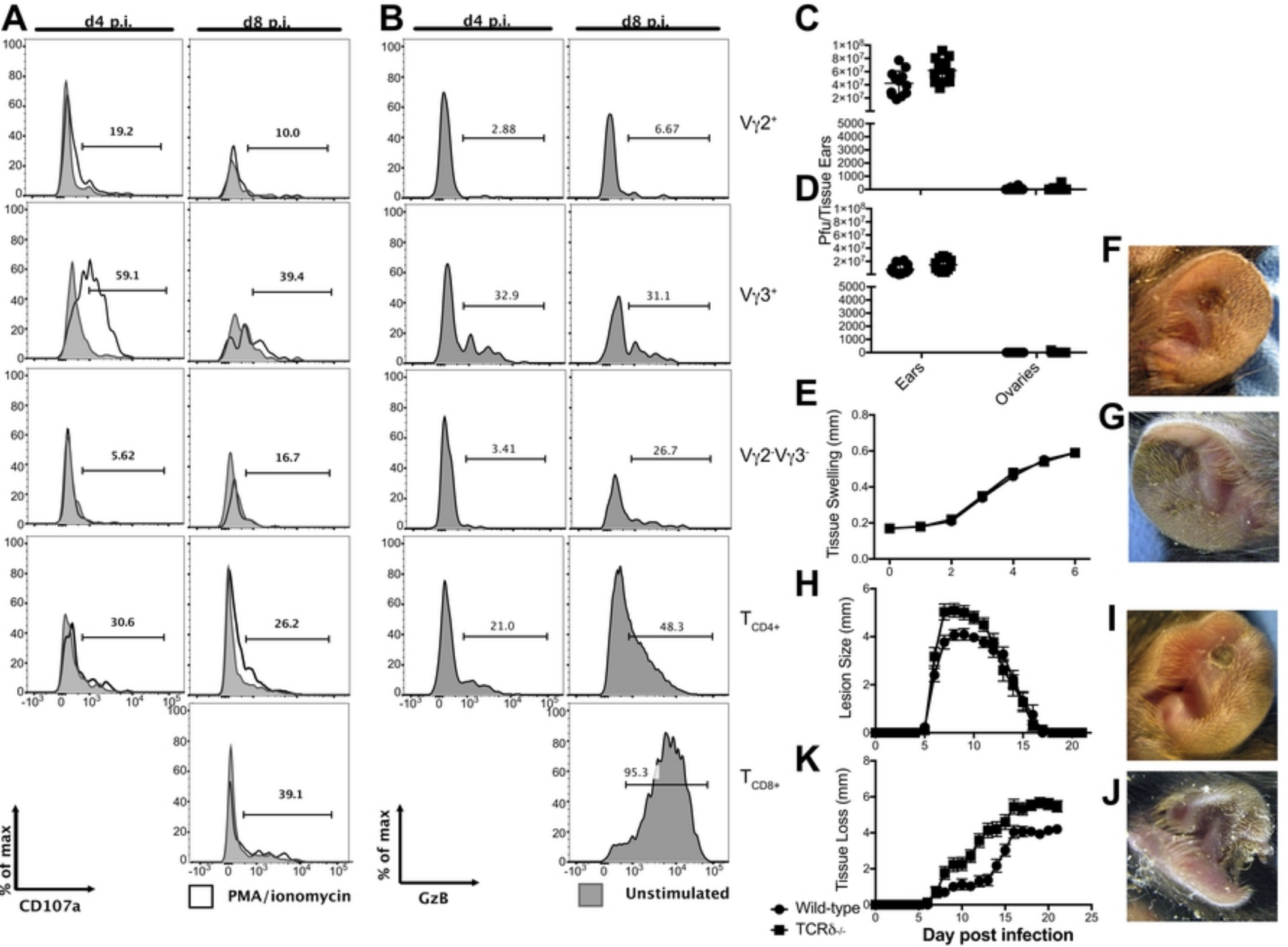
A
d4 p.i.
d8 p.i.
19.2
10.0
59.1
39.4
5.62
16.7
30.6
26.2
39.1
% of max
CD107a
PMA/ionomycin
B
d4 p.i.
d8 p.i.
2.88
6.67
32.9
31.1
3.41
26.7
21.0
48.3
95.3
% of max
GzB
Unstimulated
Vγ2+
Vγ3+
Vγ2-Vγ3-
TCD4+
TCD8+
C
Pfu/Tissue Ears
D
Ears
Ovaries
E
Tissue Swelling (mm)
F
G
H
Lesion Size (mm)
I
K
Tissue Loss (mm)
J
Wild-type
TCRδ-/-
Day post infection

Figure 2

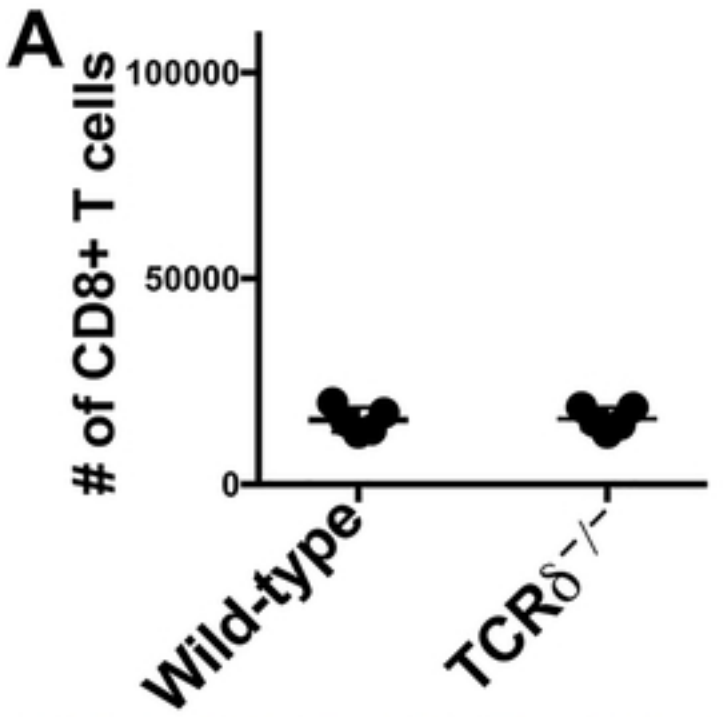

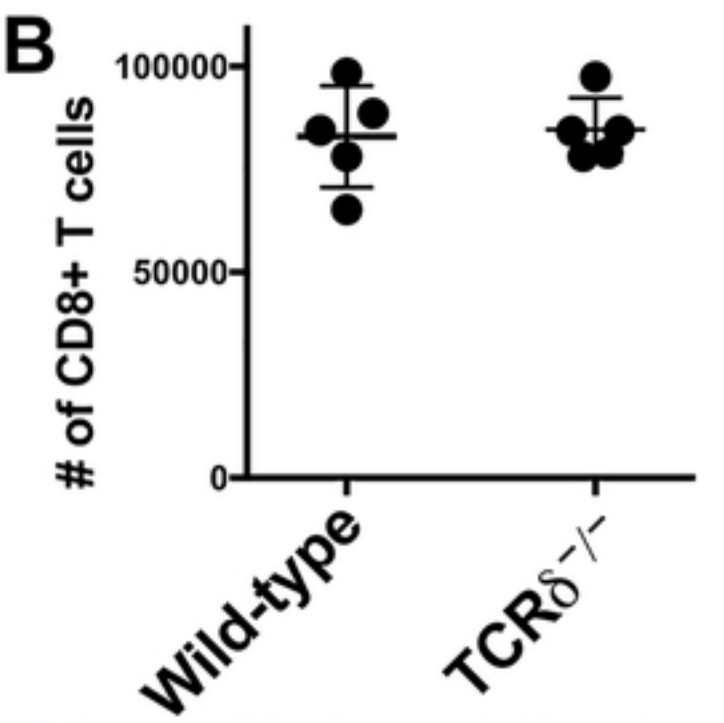

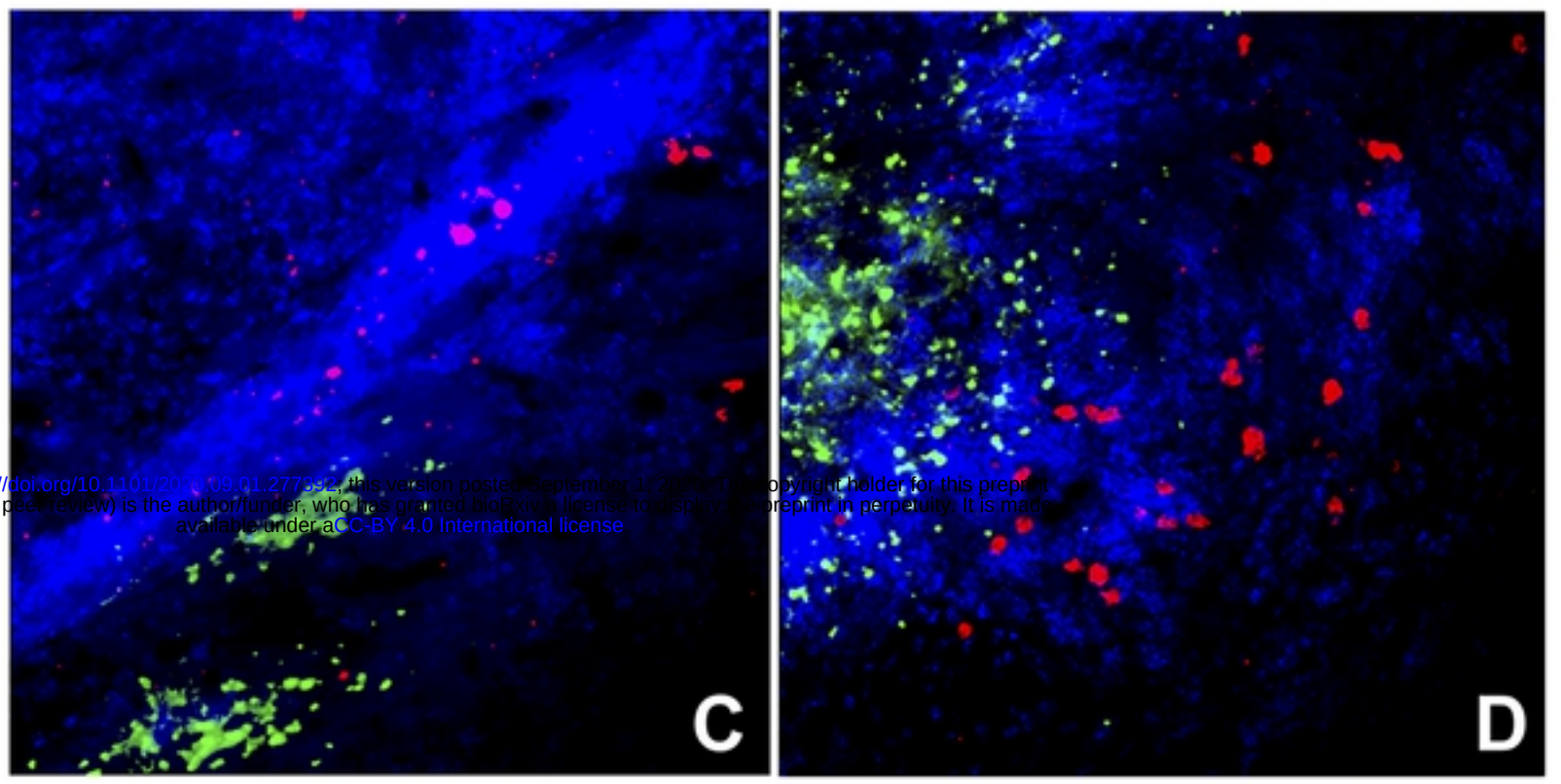

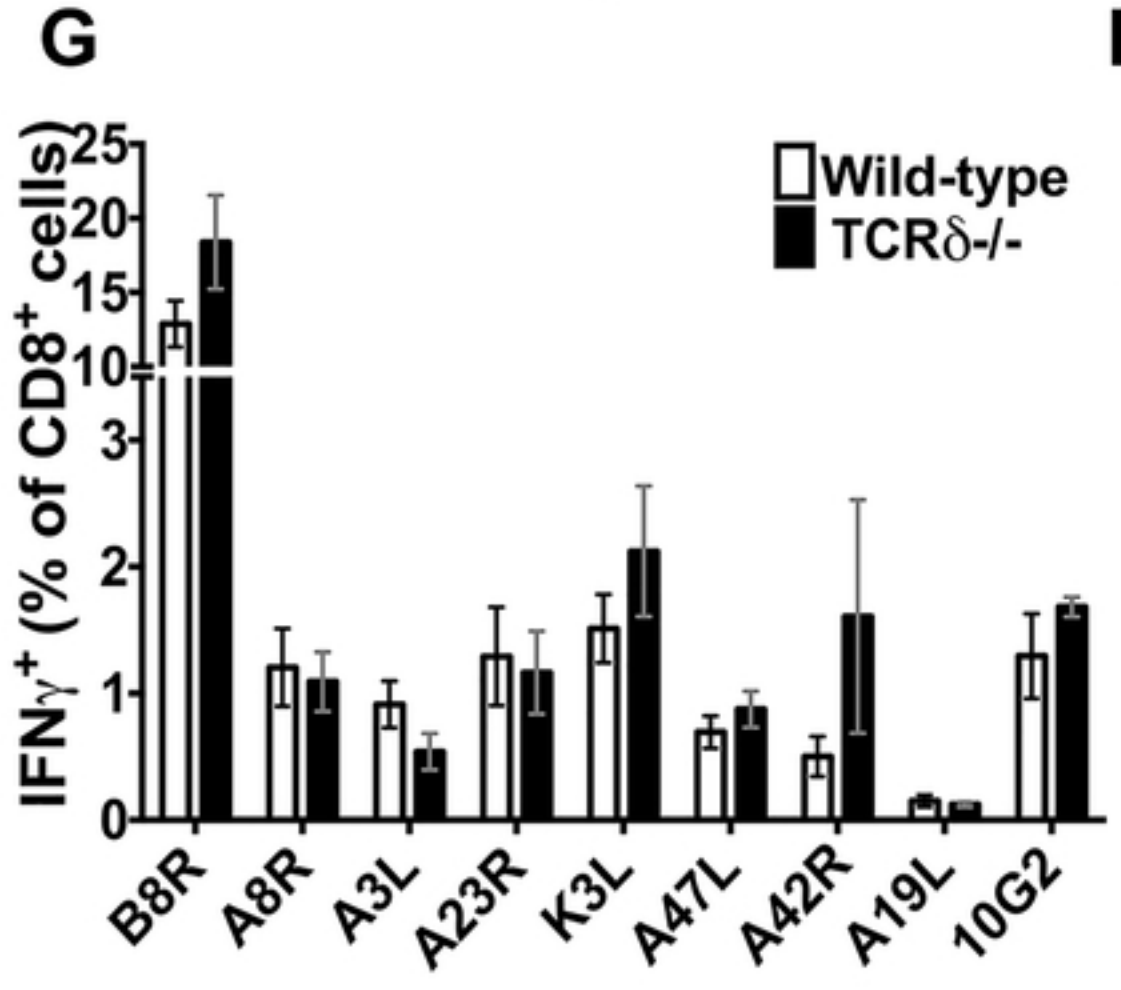

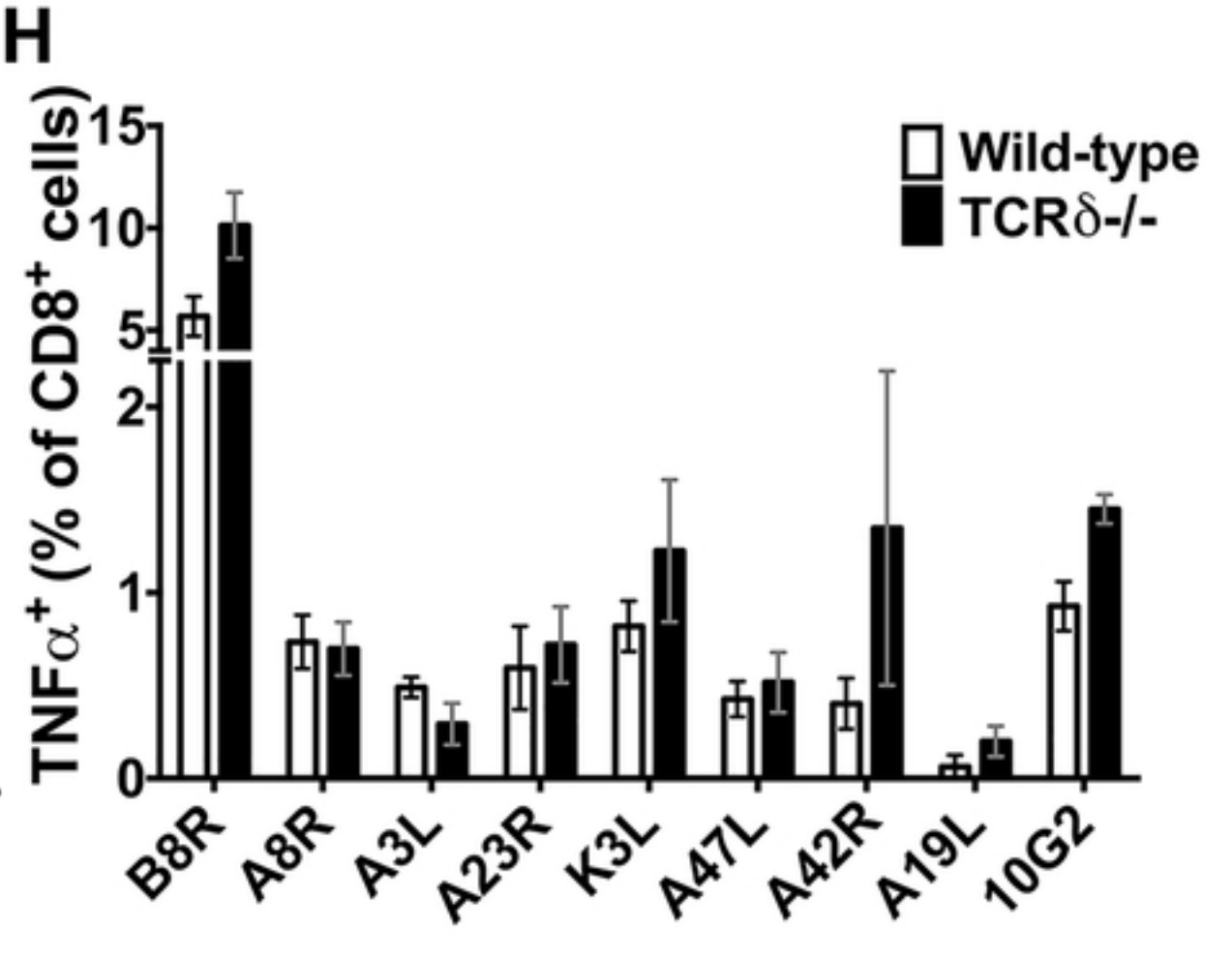

Figure 3

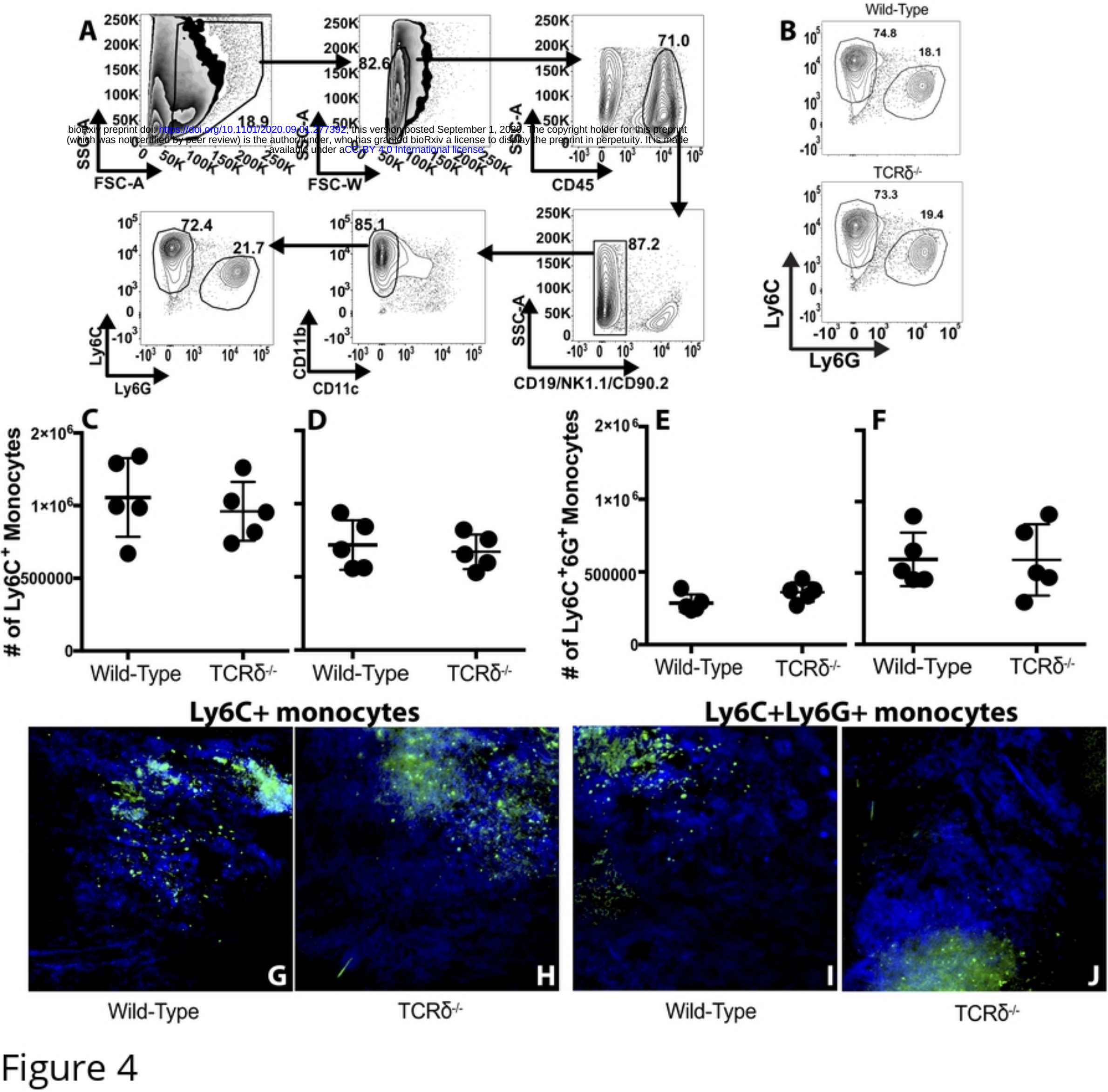

Figure 4

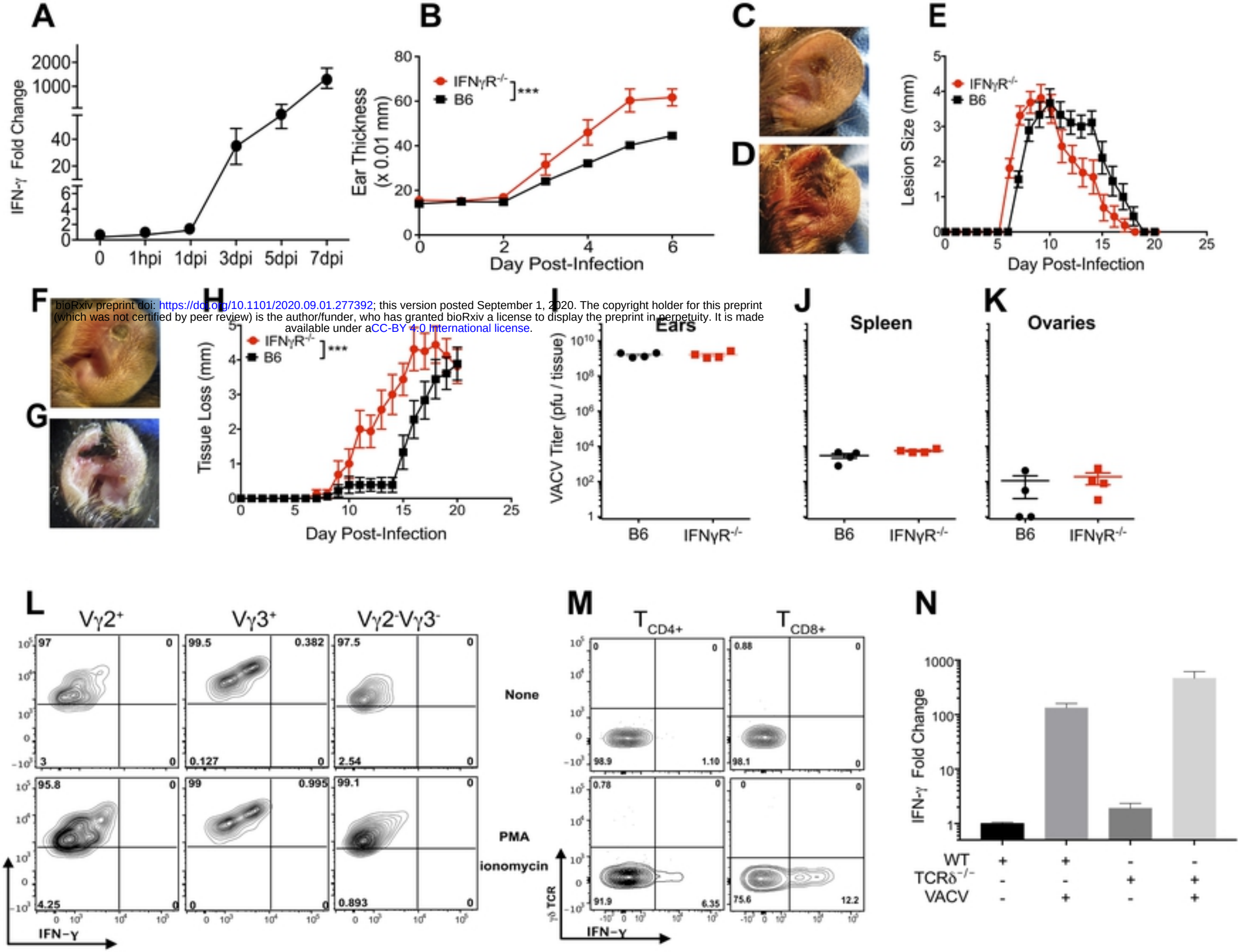

Figure 5

Figure 6

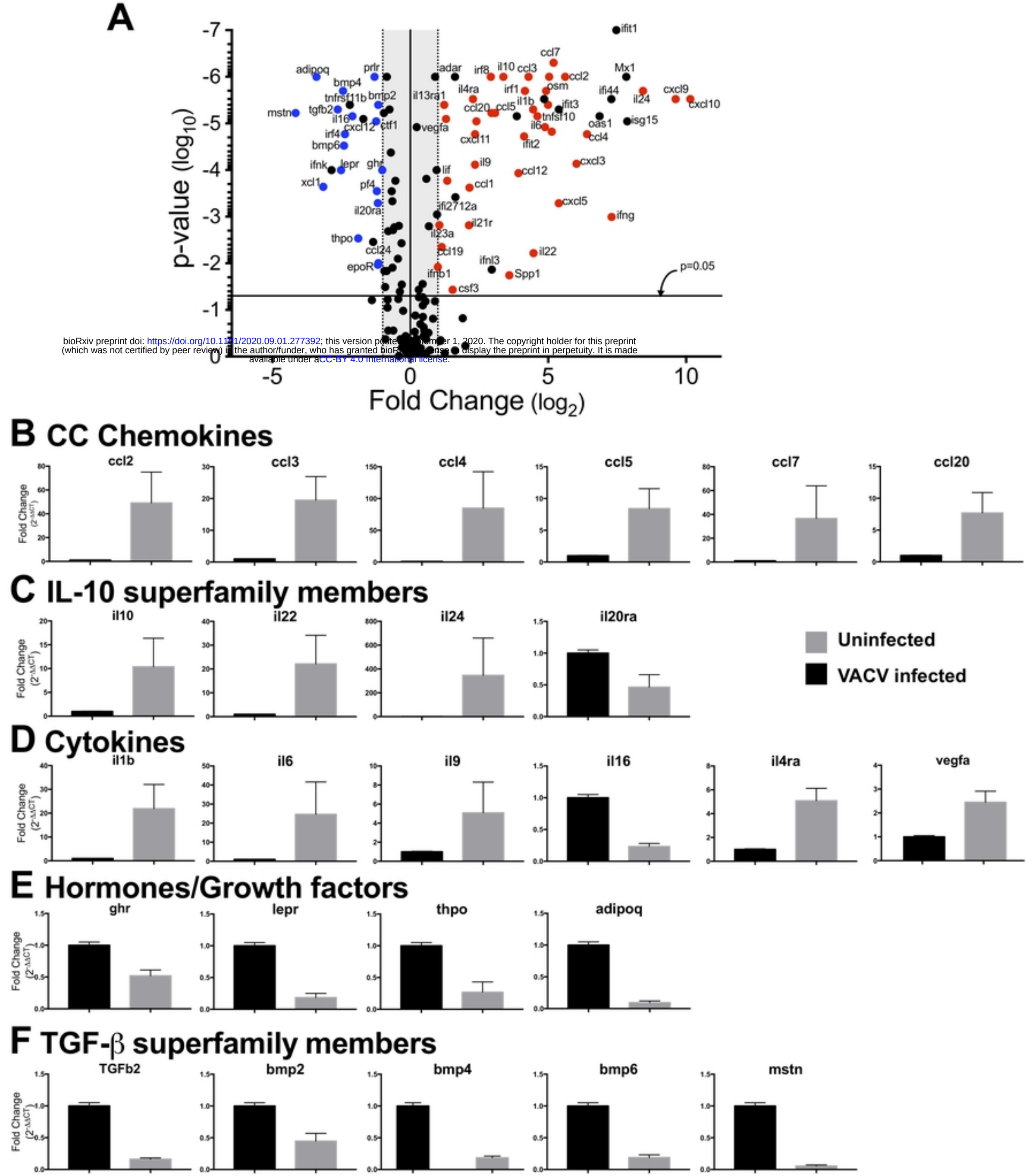

Figure 7

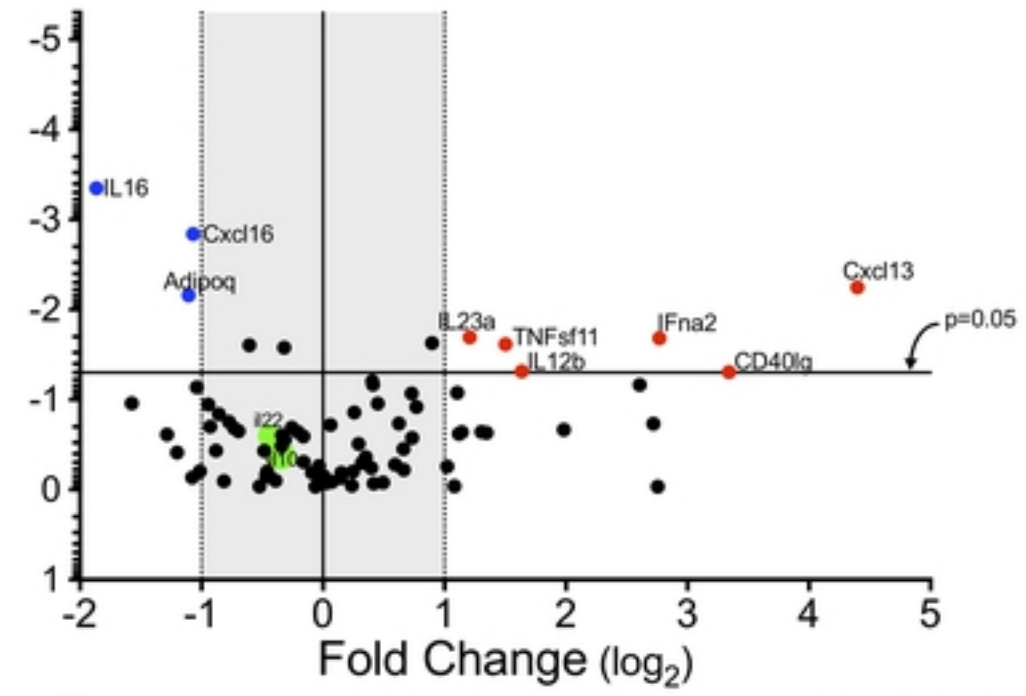

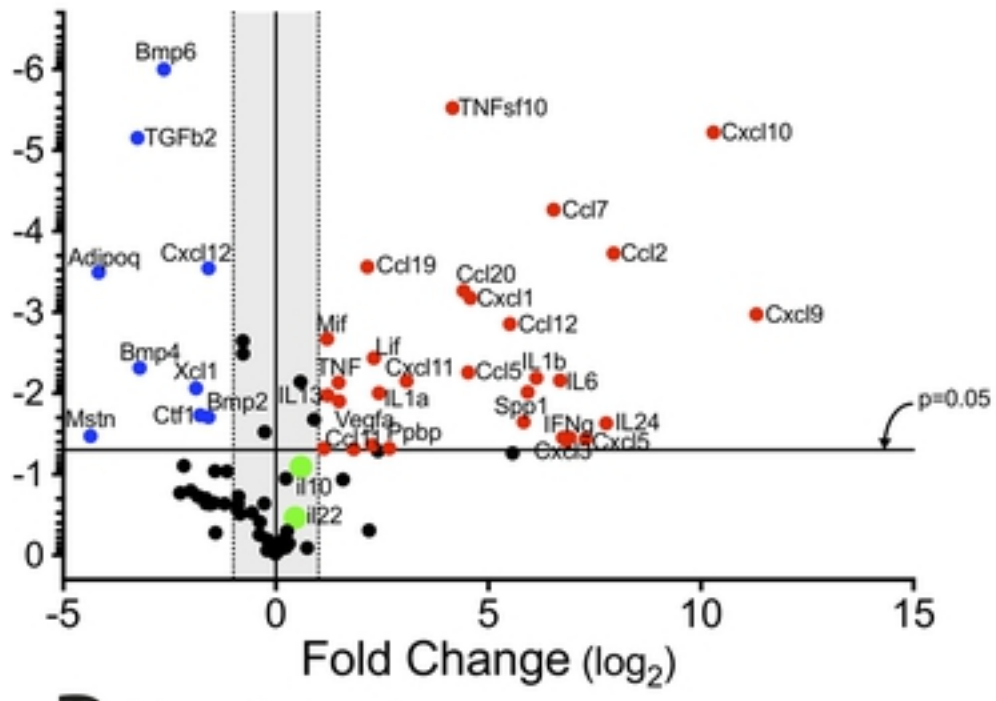

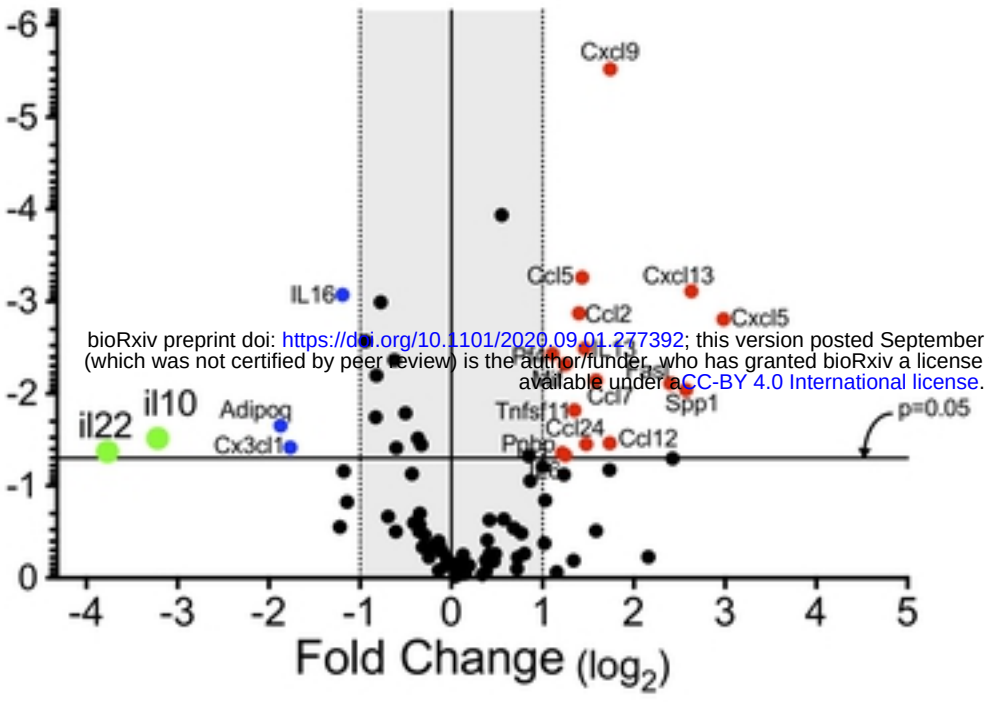

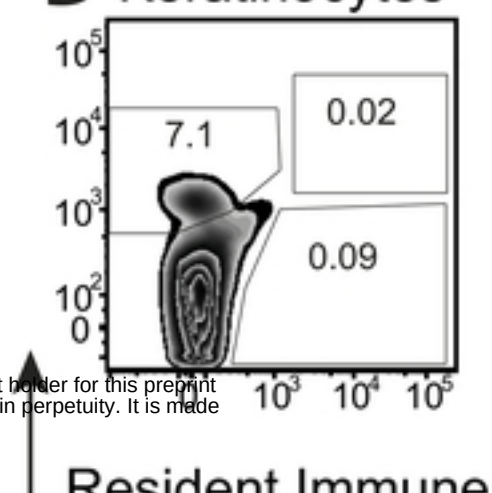

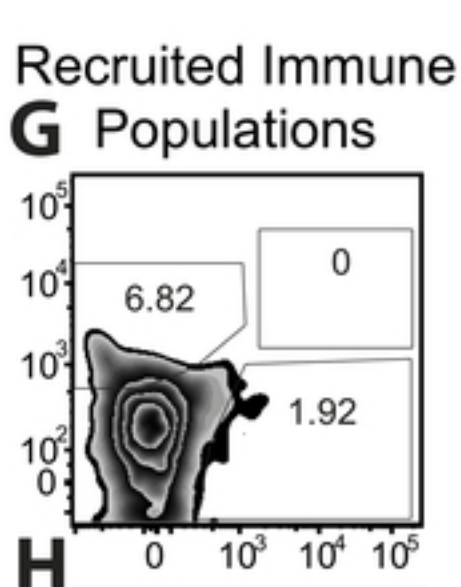

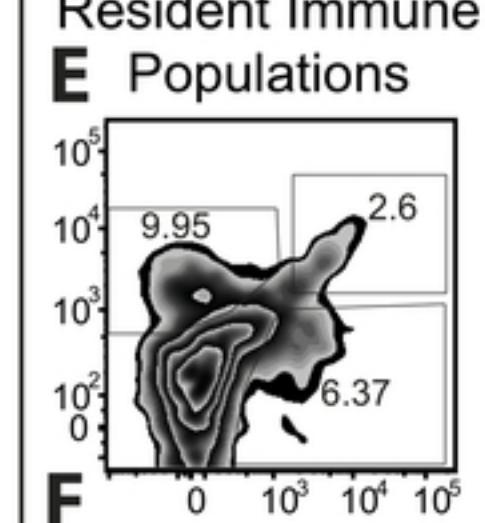

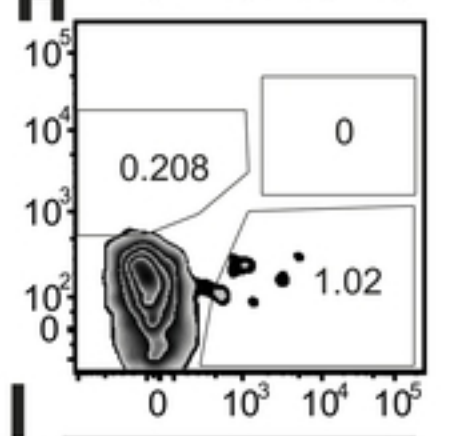

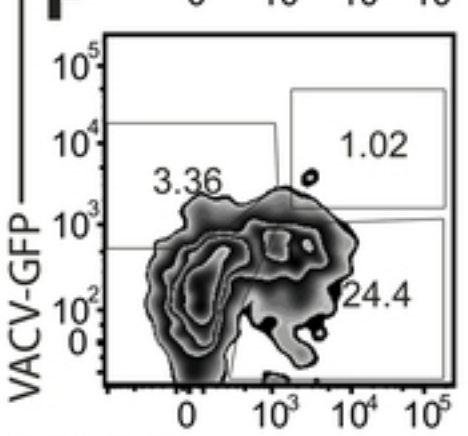

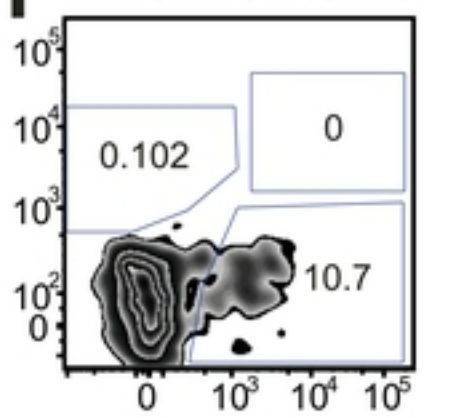

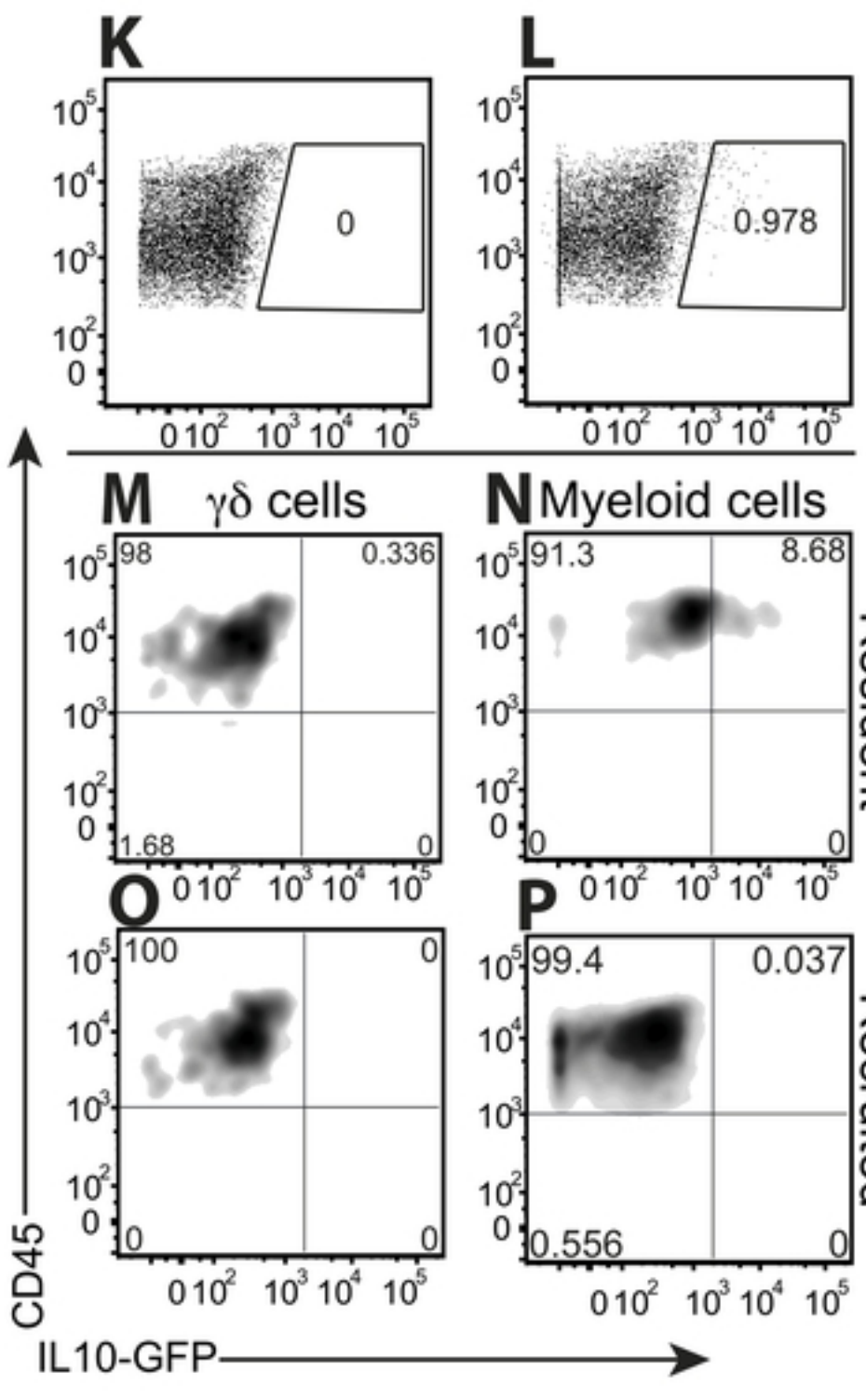

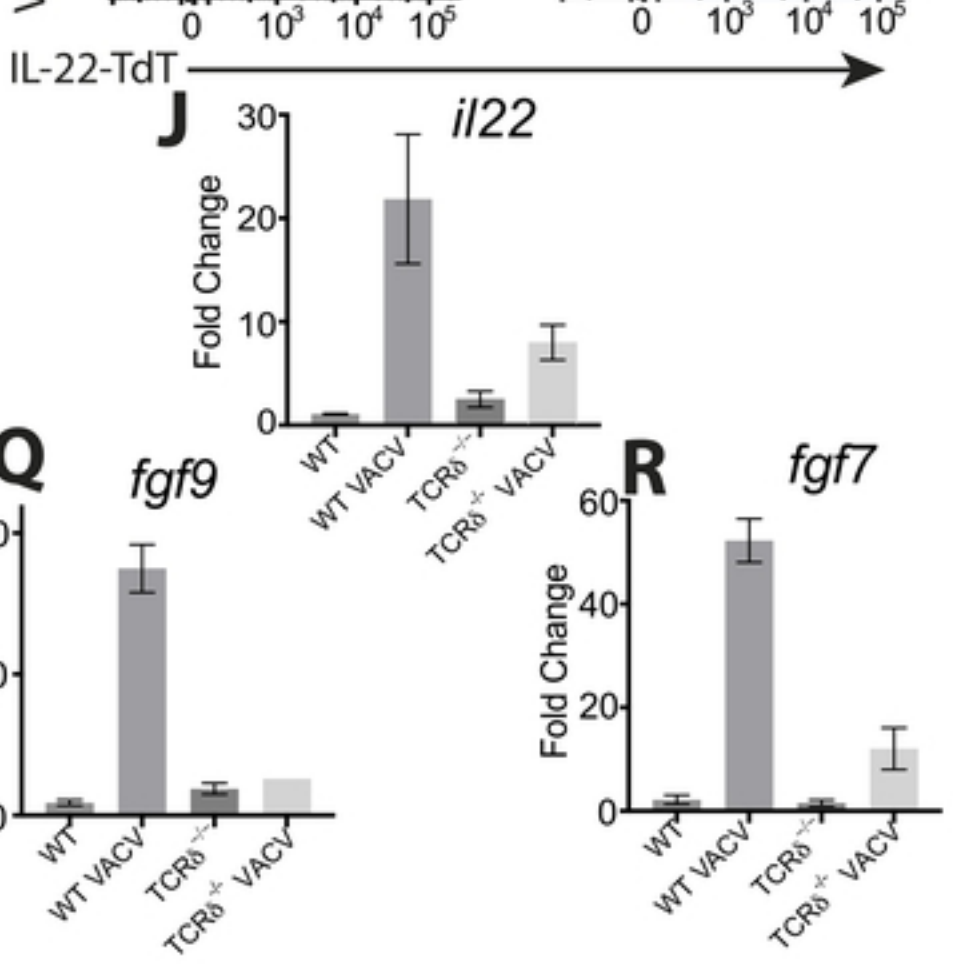

Figure 8